Title
Genetic analysis of acoustic neuromas

Author
Frazer, Kelly Ann

Publication Date
1993

Peer reviewed|Thesis/dissertation

Genetic Analysis of Acoustic Neuromas

by

Kelly Ann Frazer

DISSERTATION

Submitted in partial satisfaction of the requirements for the degree of

DOCTOR OF PHILOSOPHY

in

Anatomy

in the

GRADUATE DIVISION

of the

UNIVERSITY OF CALIFORNIA

San Francisco

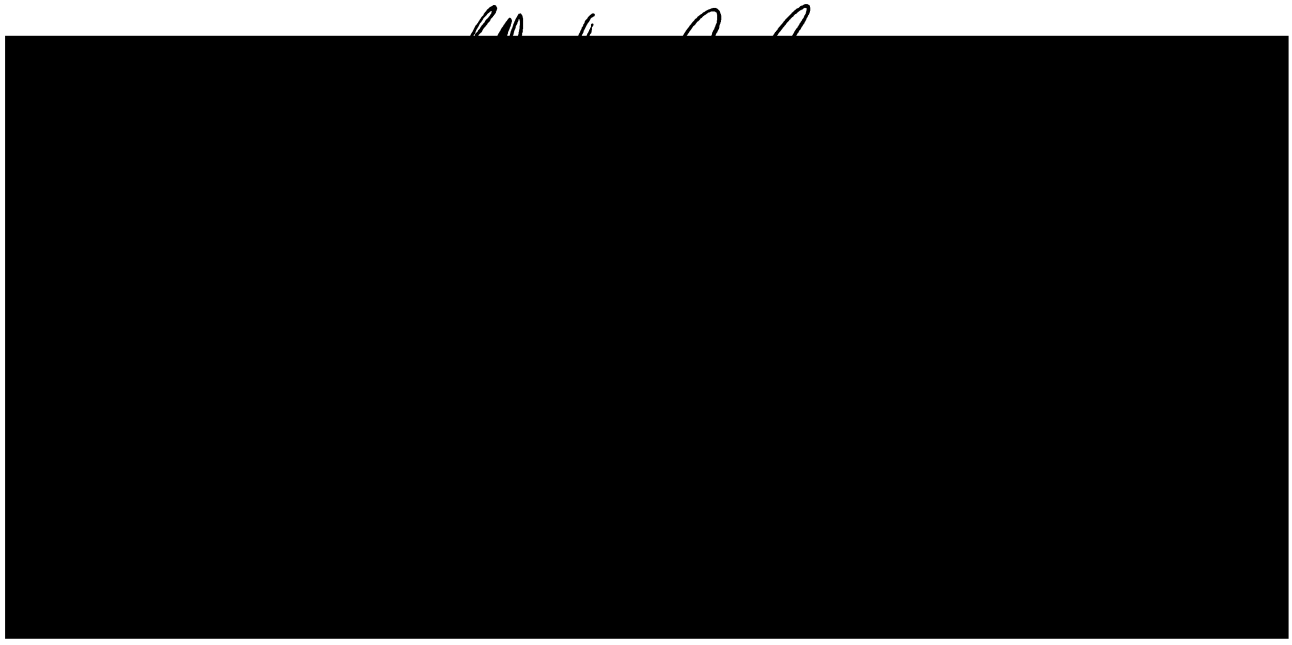

I dedicate this dissertation to my parents
Charles R. Frazer and Frances M. Frazer

Preface and Acknowledgements

I would like to give my thanks to Dr. David Cox for the time and effort spent teaching me how to be a scientist .

I am also grateful to the following past and present members of the Cox laboratory for useful scientific discussions and for time spent teaching me techniques, Val Shieffield, Geoff Duyk, Roger Wolff and Nila Patel.

I thank my husband, Masatoshi Morita, for his company and understanding.

The text of Chapter 2 is a reprint of the material as it appeared in Genomics. It is reprinted with permission from Academic Press, Inc.

UNIVERSITY OF CALIFORNIA, SAN FRANCISCO

BERKELEY • DAVIS • IRVINE • LOS ANGELES • RIVERSIDE • SAN DIEGO • SAN FRANCISCO

SANTA BARBARA • SANTA CRUZ

DEPARTMENT OF ANATOMY
SCHOOL OF MEDICINE
SAN FRANCISCO, CALIFORNIA 94143-0452
(415) 476-1861 FAX # (415) 476-4845

APR 21 1993
APR 26 1993

Liz Pope
Rights and Permission
Production Department, Sixth Floor
1250 Sixth Avenue
San Diego, California 92101

April 15, 1993

Dear Liz,

I am writing to request permission to reproduce the following article in **Genomics** as a chapter in my Ph.D. thesis:

Frazer, K.A., Boehnke, M., Budarf, M.L., Wolff, R.K., Emanuel, B.S., Myers, R.M., and Cox, D.R. (1992). A radiation hybrid map of the region on human chromosome 22 containing the neurofibromatosis type 2 locus. *Genomics* **14:** 574-584

In addition, my thesis will be submitted to University Microfilms Inc. (UMI). Consequently, your permission letter must state that you as the copyright owner are aware the UMI may supply single copies on demand.

Sincerely,

Kelly A. Frazer

Kelly A. Frazer
Department of Anatomy
School of Medicine
University of California at San Francisco
San Francisco, California 94143-0452
Ph: (415) 476-7865
Fax: (415) 476-7389

April 27, 1993

PERMISSION GRANTED, provided that 1) complete credit is given to the source, including the Academic Press copyright notice; 2) the material to be used has appeared in our publication without credit or acknowledgement to another source and 3) if commercial publication should result, you must contact Academic Press again.

We realize that University Microfilms must have permission to sell copies of your thesis, and we agree to this. However, we must point out that we are not giving permission for separate sale of your article.

Martha Strassberger
Contracts, Rights and Permissions
Academic Press, Inc.
Orlando, FL 32887

Abstract

Genetic Analysis of Acoustic Neuromas.

Kelly A. Frazer

Acoustic neuromas are common intracranial tumors occurring in humans. The majority of acoustic neuromas arise in the general population as sporadic unilateral tumors. However, a small percentage occur as bilateral tumors in individuals with the rare hereditary syndrome known as Neurofibromatosis Type 2 (NF 2). Analyses of sporadic and hereditary acoustic neuromas have shown that specific loss of chromosome 22 DNA material frequently occurs in these tumors. These data suggest that both sporadic and inherited acoustic neuromas most likely result from inactivation of the same genetic locus. However, it is also possible that two separate loci, one responsible for the inherited predisposition and the other involved in the formation of sporadic tumors, are located in close proximity to one another on chromosome 22.

In order to identify genes involved in the development of acoustic neuromas, I analyzed sporadic tumors for chromosome 22 rearrangements. The strategy was to first identify the locus involved in the development of sporadic acoustic neuromas by determining the smallest common region of deletions in these tumors. Next, tumor DNA and blood DNA from NF 2 patients would be analyzed for mutations at this locus to determine if the same gene was involved in the formation of hereditary acoustic neuromas.

As an initial step to identify genes involved in the development of acoustic neuromas on chromosome 22, I constructed a 500 kb resolution radiation

hybrid map of the NF 2 region between the markers, D22S1 to D22S28. This radiation hybrid map was used to localize chromosome 22 rearrangements in sporadic tumors. Secondly, I developed an approach to efficiently analyze acoustic neuromas for chromosomal rearrangements that involves generating hamster-tumor hybrid cell lines. These hybrid cell lines immortalize the chromosome 22 DNA from the tumors, which allows one to karyotype the chromosomes and provides an unlimited source of material for molecular analysis.

These approaches allowed me to identify an acoustic neuroma that is monosomic for chromosome 22 and contains a reciprocal translocation in the remaining chromosome 22 homolog. Radiation hybrid mapping localized the translocation breakpoint to a 250 kb region of chromosome 22 between DNA markers D22S347 and D22S349. This region is approximately 2 Mb distal to the Merlin gene, a recently described candidate for the NF 2 tumor suppresser locus. Our results suggest that more than one chromosome 22 locus is involved in the development of acoustic neuromas.

Table of Contents

List of Tables

List of Figures

Chapter 4

Chapter 1

Introduction

Acoustic neuromas, the commonly used term for Schwannomas of the eighth cranial nerve, account for approximately 8 percent of all intracranial tumors (Jackler and Pitts 1990). The majority of acoustic neuromas arise in the general population as sporadic unilateral tumors. However, approximately 5 percent of acoustic neuromas occur as bilateral tumors in individuals with the rare hereditary syndrome known as Neurofibromatosis Type 2 (NF2) (Jackler and Pitts 1990). In addition to bilateral acoustic neuromas, NF2 patients frequently develop other types of nervous system tumors, including meningiomas, gliomas, and spinal neurofibromas.

At the time I began my dissertation research, genetic linkage analysis in a large extended family had identified significant linkage between the NF 2 genetic disorder and a polymorphic marker on chromosome 22 (Rouleau et al. 1987). Comparisons between tumor DNA and blood DNA in NF 2 patients showed that specific loss of chromosome 22 DNA frequently occurs in hereditary acoustic neuromas (Seizinger et al. 1987b, Fontaine et al. 1991, Wolff et al. 1992). Similar analysis of sporadic acoustic neuromas and meningiomas also demonstrated specific loss of chromosome 22 DNA (Seizinger et al. 1986, Fontaine et al. 1991, Wolff et al. 1992). These data suggested that the NF 2 locus is a recessive tumor suppressor gene involved in the development of hereditary and sporadic NF 2-related tumors (Seizinger et al. 1986, 1987a, 1987b).

My dissertation research involved the development and application of new technology in an effort to isolate the NF 2 gene, using an approach commonly referred to as positional cloning (Collins, 1992). Positional cloning is a strategy that identifies and isolates mutant genes involved in the development of inherited single gene disorders, based on their chromosomal location. Since

the mutant loci are isolated on the basis of their genetic/physical position in the genome, prior knowledge about the biochemical or physiological properties of the disease gene products and their role in the genetic disorder is not necessary.

In positional cloning, the disease locus is first localized to a specific region in the human genome by genetic linkage analysis of pedigrees segregating the disorder. Next the DNA between the flanking markers of the disease gene is cloned, and then all the transcribed genes in the region are isolated and analyzed for mutations in individuals with the genetic disorder. A locus is considered a likely candidate for the disease gene if it contains alterations specifically associated with the genetic disorder.

At the time I initiated my dissertation research, very few human disease genes had been successfully isolated using the positional cloning approach. In practice, it was difficult to localize a disease gene in the human genome because the available genetic linkage maps lacked highly informative markers evenly spaced along the chromosomes. Over the past few years, efforts to develop a high resolution linkage map of the human genome have resulted in maps, with relatively high marker density and numerous informative loci, for each of the 23 pairs of chromosomes (NIH/CEPH Collaborative Mapping Group, 1992). These currently available genetic maps span at least 92 % of the genome and therefore can be used to localize most disease genes. However, genetic linkage mapping is still limited by the number of informative meiosises in the pedigrees segregating the disorder. For most genetic disorders, the number of informative meiosises available is usually between 10 and 100; therefore genetic linkage analysis usually localizes a disease locus to a genetic

interval of 1 to 10 centimorgans (cM), which corresponds to approximately 1 to 10 million base pairs (Mb).

Six years ago, after a disease gene was localized by linkage analysis, a tremendous amount of effort was required to isolate the DNA between the flanking markers. The current availability of human yeast artificial chromosome (YAC) libraries, containing clones with large inserts, has greatly facilitated the ability to isolate large segments of genomic DNA. A YAC contig spanning the region between the flanking markers of a disease gene provides the necessary cloned materials for the identification of the transcribed genes in the region.

Several new strategies, including exon amplification (Buckler et al., 1991), exon trapping (Duyk et al., 1990) and using YACs as probes to screen cDNA libraries directly, are capable of isolating the majority of the genes in a candidate region relatively easily. However, in order to identify the disease gene, it is necessary to analyze all the isolated genes for mutations in individuals with the genetic disorder. This approach is quite a laborious process for megabase-sized candidate regions. By contrast, the availability of either cytogenetic or molecular rearrangements associated with a genetic disorder can precisely define the chromosomal localization of the gene and therefore greatly expedite its isolation. In fact, almost all of the disease genes isolated to date by positional cloning have relied on chromosomal rearrangements, such as translocations, deletions, and trinucleotide repeat expansions, which are detectable by using Southern blot analysis. The strategy used to isolate the majority of these disease genes has relied on obtaining a probe that identified restriction fragments altered by the chromosomal rearrangement. To find transcribed sequences affected by the chromosomal

rearrangement, such probes are used to directly screen cDNA libraries, or as a reagent to isolate cloned trapped exons by exon amplification.

At the time I began my dissertation research, the majority of the reagents and techniques currently used for constructing genetic linkage maps, physical maps, isolating large segments of genomic DNA, and identifying candidate genes were not available. Through my efforts to isolate the NF 2 gene based on its chromosomal position, I helped establish several of the current techniques used for constructing physical maps, analyzing solid tumors for chromosomal rearrangements, and isolating large genomic regions in overlapping DNA clones. In addition, my analysis of NF 2-related tumors has suggested that two separate chromosome 22 loci separated by approximately 2 Mb of DNA may be involved in the development of acoustic neuromas. Specifically my dissertation research addressed the following issues:

1. Construction of a physical map at the 500 kilobase level of resolution of the NF 2 region on chromosome 22.

Just after I began my dissertation research, a study was published that had localized the NF 2 locus within a 13 cM region on the long arm of chromosome 22, between the DNA markers D22S1 and D22S28 (Rouleau et al., 1990). To further refine the position of the NF 2 gene, two approaches were available: linkage analysis of NF 2 families and deletion analysis of sporadic and inherited NF 2 associated tumors. Due to the rarity of the disorder, very few NF 2 families large enough to obtain additional information about the location of the NF 2 gene by linkage analysis were available. However, because acoustic neuromas compose a large percentage of the sporadically-occurring central nervous system tumors, a large number of these tumors are available for study.

Therefore, I decided to further localize the position of the NF 2 gene on chromosome 22 by determining the smallest common region of deletions in sporadic acoustic neuromas. The basic assumption underlying this deletion analysis approach is that inherited and sporadic acoustic neuromas result from inactivation of the same genetic locus. At the time, we did not know if this assumption was valid or not. We discussed the possibility that the chromosome 22 rearrangements observed in acoustic neuromas may result from two separate genetic loci, one responsible for the inherited predisposition and the other involved in the formation of sporadic tumors. If this were the case, we realized that the deletion analysis approach that I decided to use would not result in the isolation of the NF 2 gene but instead would identify a genetic locus involved in the development of sporadic acoustic neuromas.

To analyze the acoustic neuromas for chromosomal rearrangements, it was necessary to construct a high-resolution map of the region between D22S1 and D22S28 on chromosome 22. High-resolution maps are not easily generated by genetic linkage analysis because in molecular terms their resolution is low, and only a limited number of the available markers that recognize polymorphisms can be mapped. For example, construction of a 1 cM genetic interval map of the 13 cM NF 2 region would have required analyzing an estimated 130 meiosis with approximately 30 informative polymorphic probes. The technique of pulse field gel electrophoresis (PFGE), which allows the separation of small and large DNA fragments, provides a method of producing long-range physical maps several megabase pairs in size. A physical map is constructed by first cleaving genomic DNA with restriction enzymes that cut infrequently in human DNA and then separating the DNA fragments, usually hundreds of kilobases in length, in agarose gels. The DNA fragments separated on the gels are probed with

markers which are then ordered relative to each other based on their recognition of restriction fragments of the same length. However, it is difficult to construct maps more than a few hundred kilobases in length using PFGE because the rare cutter sites are non-randomly distributed in the human genome and there are only a limited number of rare cutter enzymes. Thus, in practice, the inability to easily construct maps of the human genome at the 100 - 500 kilobase level of resolution is a major problem encountered in using the positional cloning approach to isolate disease genes.

In order to overcome some of the difficulties in constructing a map of the human genome at the 500 kilobase level of resolution, I helped develop a somatic cell genetic mapping approach known as radiation hybrid (RH) mapping. In chapter 2, I describe the use of RH mapping to generate a map at the 500 kilobase level of resolution of the region on chromosome 22 between BCR2L and PDGFB.

2. Analysis of acoustic neuromas for chromosomal rearrangements.

After I generated the RH map of the NF 2 region on chromosome 22, I used this map to search for chromosomal rearrangements in sporadic acoustic neuromas. Most prior studies involving the analysis of acoustic neuromas for chromosome 22 rearrangements have used polymorphic markers to compare tumor DNA with blood DNA from single patients to identify the loss of chromosome 22 alleles (Seizinger et al. 1986, 1987b, Fontaine et al. 1991, Bijlsma et al. 1992, Wolff et al. 1992). This type of analysis has been limited by the degree of polymorphism of available chromosome 22 markers as well as by the fact that this approach only detects those chromosomal rearrangements that

result in deletions and monosomy. While other types of chromosomal rearrangements, such as translocations and inversions, could be detected by cytological analysis of the tumors, acoustic neuromas grow poorly in culture, are contaminated with non-tumor cells and thus are difficult to karyotype accurately (Rey et al. 1987, Couturier et al. 1990). In addition, analysis of acoustic neuromas for chromosome 22 rearrangements are often limited by the small amount of material available from each tumor.

In order to solve these problems, I developed an approach for tumor analysis that involves fusing tumor cells with an established hamster cell line to generate hamster-tumor hybrid cell lines. In Chapter 3, I describe how the resulting hamster-tumor hybrids immortalize the chromosome 22 sequences from the tumors, which allows the chromosomes to be karyotyped and provides an unlimited source of material for molecular analysis.

3. The possibility that two separate genetic loci, one responsible for the development of inherited acoustic neuromas and the other involved in the formation of sporadic acoustic neuromas, may lie approximately 2 Mb apart from one another on chromosome 22.

Based on studies of constitutional chromosome 22 rearrangements in a number of different NF2 patients, a candidate gene for the NF2 tumor suppressor locus was recently identified (Trofatter et al. 1993). This candidate gene, Merlin, is currently being analyzed for mutations in hereditary and sporadic acoustic neuromas. Preliminary data has indicated that the Merlin gene is not rearranged in all sporadic acoustic neuromas (R.K. Wolff, personal communication), suggesting that other chromosome 22 genes are involved in the development of these tumors.

In Chapter 3, I describe the analysis of a sporadic acoustic neuroma that has lost one chromosome 22 homolog and contains a translocation approximately 2 Mb distal to the Merlin gene on the copy of chromosome 22 remaining in the tumor. Sequence analysis indicates that the primary structure of the Merlin gene in the tumor is not mutated (R.K. Wolff, unpublished data). Other workers have also reported chromosomal rearrangements in acoustic neuromas and a meningioma (Zhang et al. 1990, Ahmed et al 1991), located approximately 2 Mb distal to the Merlin gene. These data suggest that two separate chromosome 22 genetic loci, the Merlin gene and a locus affected by the translocation, may be involved in the development of acoustic neuromas.

4. Isolation of DNA clones in the genomic region between D22S347 and D22S349.

After characterizing the sporadic acoustic neuroma containing the chromosome 22 translocation, I attempted to isolate the genetic locus affected by the breakpoint. The positional cloning strategy of isolating genes generally relies on cloning large regions of genomic DNA between the two flanking marker loci. In this case, the closest flanking DNA markers of the translocation breakpoint, D22S347 and D22S349, are separated by approximately 250 kb. The ability to clone segments of genomic DNA of this size has been greatly facilitated by the development of human YAC libraries, which contain clones with large DNA inserts. A YAC contig spanning the region between the flanking loci, D22S347 and D22S349, would provide the necessary cloned materials for the identification of the breakpoint. However, YAC clones are often difficult to analyze and manipulate. A major problem in using YACs is that approximately fifty percent of the clones in most libraries are chimeric, such that a considerable

amount of DNA in a set of overlapping YAC clones is not from the genomic region under study. In addition, isolating DNA directly from YACs is time consuming and usually only small quantities of DNA are obtained.

In Chapter 4, I describe how I solved these problems by converting the YAC clones isolated with STSs at the loci D22S347 and D22S349 into cosmids, which are more easily analyzed and manipulated. Since the YACs were used as probes to directly screen a sub-chromosome 22 specific cosmid library, I only required small quantities of YAC DNA and was quickly able to access the chromosome 22 DNA present in the chimeric YAC clones.

References:

Ahmed FB, Maher ER, Affara NA, Bentley E, Xuereb JH, Rouleau GA, Hardy D, David M, Ferguson-Smith MA (1991) Deletion mapping in acoustic neuroma. Cytogenet Cell Genet HGM11:203

Bijlsma EK, Brouwer-Mladin Roma, Bosch DA, Westerveld A, Hulsebos TJM (1992) Molecular characterization of chromosome 22 deletions in schwannomas. Genes Chromosom Cancer 5:201-205

Buckler AJ, Chang DD, Graw SL, Brook JD, Haber DA, Sharp PA, Housman DE (1991) Exon amplification : a strategy to isolate mammalian genes based on RNA splicing. Proc Natl Acad Sci USA 88:4005-4009.

Collins FS (1992) Positional cloning: Let's not call it reverse anymore. Nature Genetics 1:3-6

Couturier J, Delattre O, Kujas M, Philippon J, Peter M, Rouleau G, Aurias A, Thomas G (1990) Assessment of chromosome 22 anomalies in neurinomas by combined karyotype and RFLP analyses. Cancer Genet Cytogenet 45:55-62

Duyk GM, Kim s, Myers RM, Cox DR (1990) Exon trapping: A genetic screen to identify candidate transcribed sequences in clones mamalian genomic DNA. Proc Natl Acad Sci USA 87:8995-8999.

Fontaine B, Sanson M, Delattre O, Menon AG, Rouleau GA, Seizinger BR, Jewell AF, Hanson MP, Aurias A, Martuza RL, Gusella JF, Thomas G (1991) Parental origin of chromosome 22 loss in sporadic and NF2 neuromas. Gemonics 10:280-283

Jackler RK, Pitts LH (1990) Acoustic Neuroma. Neurosurg Clin North Am 1:199-223

Rey JA, Bello MJ, de Campos JM, Kusak E, Moreno S (1987) Cytogenetic analysis in human neurinomas. Cancer Genet Cytogenet 28:187-188

Rouleau GA, Seizinger BR, Wertelecki W, Haines JL, Superneau DW, Martuza RL, Gusella JF (1990) Flanking markers bracket the neurofibromatosis type 2 (NF2) gene on chromosome 22. Am J Hum Genet 46:323-328

Rouleau GA, Wertelecki W, Haines JL, Hobbs WJ, Trofatter JA, Seizinger BR, Martuza RL, Superneau DW, Connealy PM, Gusella JF (1987) Genetic linkage of bilateral acoustic neurofibromatosis to a DNA marker on chromosome 22. Nature 329:246-248

Seizinger BR, de la Monte S, Atkins L, Gusella JF, Martuza RL (1987a) Molecular genetic approach to human meningioma: loss of genes of chromosome 22. Proc Natl Acad Sci USA 84:5419-5423

Seizinger BR, Martuza RL, Gusella JF (1986) Loss of genes on chromosome 22 in tumorigenesis of human acoustic neuromas. Nature 322:644-647

Seizinger BR, Rouleau GA, Ozelius LJ, Lane AH, St George-Hyslop P, Huson S, Gusella JF, Martuza RL (1987b) Common pathogenetic mechanism for three tumor types in bilateral acoustic neurofibromatosis. Science 236:317-319

Trofatter JA, MacCollin MM, Rutter JL, Murrell JR, Duyao MP, Parry DM, Eldridge T, Kley N, Menon AG, Pulasid K, Hasse VH, Ambroae DM, Munroe D, Bove C, Haines JL, Martuza RL, MacDonald ME, Seizinger BR, Short MP, Buckler AJ, Gusella JF (1993) A novel moesin-, exrin-, radixim-like gene is a candidate for the neurofibromatosis 2 tumor suppressor. Cell 72: 791-800

Wolff RK, Frazer KA, Jackler RK, Lanser MJ, Pitts LH, Cox DR (1992) Analysis of chromosome 22 deletions in neurofibromatosis type2-related tumors. Am J Hum Genet 51:478-485

Zhang FR, Delattre O, Rouleau G, Couturier J, Lefrancoid D, Thomas G, Aurias A (1990) The neuroepithelioma breakpoint on chromosome 22 is proximal to the meningioma locus. Genomics 6:174-177

Chapter 2

A Radiation Hybrid Map of the Region on Human Chromosome 22 Containing the Neurofibromatosis Type 2 Locus

Genomics 14, 574-584

GENOMICS 14, 574–584 (1992)

A Radiation Hybrid Map of the Region on Human Chromosome 22 Containing the Neurofibromatosis Type 2 Locus

KELLY A. FRAZER,* MICHAEL BOEHNKE,† MARCIA L. BUDARF,‡ ROGER K. WOLFF,§ BEVERLY S. EMANUEL,‡ RICHARD M. MYERS,||,¶ AND DAVID R. COX§,¶,[1]

*Departments of *Anatomy, §Psychiatry, ¶Biochemistry and Biophysics, and ||Physiology, University of California, San Francisco, California, 94143; ‡Pediatrics and Human Genetics, University of Pennsylvania School of Medicine and Children's Hospital of Philadelphia, Philadelphia, Pennsylvania 19104; and †Biostatistics, School of Public Health, University of Michigan, Ann Arbor, Michigan 48109*

Received January 30, 1992; revised July 20, 1992

We describe a high-resolution radiation hybrid map of the region on human chromosome 22 containing the neurofibromatosis type 2 (NF2) gene. Eighty-five hamster–human somatic cell hybrids generated by X-irradiation and cell fusion were used to generate the radiation hybrid map. The presence or absence of 18 human chromosome 22-specific markers was determined in each hybrid by using Southern blot hybridization. Sixteen of the 18 markers were distinguishable by X-ray breakage in the radiation hybrids. Analysis of these data using two different mathematical models and two different statistical methods resulted in a single framework map consisting of 8 markers ordered with odds greater than 1000:1. The remaining nonframework markers were all localized to regions consisting of two adjoining intervals on the framework map with odds greater than 1000:1. Based on the RH map, the NF2 region of chromosome 22, defined by the flanking markers D22S1 and D22S28, is estimated to span a physical distance of approximately 6 Mb and is the most likely location for 9 of the 18 markers studied: D22S33, D22S41, D22S42, D22S46, D22S56, LIF, D22S37, D22S44, and D22S15. © 1992 Academic Press, Inc.

INTRODUCTION

Neurofibromatosis type 2 (NF2) is an autosomal dominant disorder associated with the development of bilateral acoustic neuromas and other nervous system tumors, including meningiomas, gliomas, and neurofibromas. The growth of these tumors in patients with NF2 can have severe consequences, leading to deafness, vertigo, paresis, and death in the third to fourth decade of life (Martuza and Eldridge, 1988). The observation of common nonrandom loss and structural rearrangements of chromosome 22 in acoustic neuromas and meningiomas first suggested that the NF2 gene might be present on this chromosome (Zankl and Zang, 1972; Seizinger *et al.*, 1986, 1987). More recently, tumor deletion studies and genetic linkage analyses have indicated that the NF2 locus is a tumor suppressor gene located within a 13-cM region on the long arm of chromosome 22, between the flanking markers D22S1 and D22S28 (Rouleau *et al.*, 1990). Genetic linkage studies have localized several polymorphic markers to the NF2 region of chromosome 22, between D22S1 and D22S28 (Rouleau *et al.*, 1989; Dumanski *et al.*, 1991). In addition, physical mapping studies have used somatic cell hybrids containing defined portions of chromosome 22 to assign a number of probes to the NF2 region (Budarf *et al.*, 1991, Delattre *et al.*, 1991). However, the orders and distances between many of these markers are not completely defined, and the published maps of the NF2 region are crude in molecular terms.

In this study we have used radiation hybrid (RH) mapping to construct a fine-structure map of the NF2 region on chromosome 22. RH mapping is a somatic cell genetic technique in which the frequency of X-ray breakage between chromosome-specific DNA markers is analyzed statistically to determine the order and distance between these markers along the chromosome (Cox *et al.*, 1990). A distinct advantage of RH mapping over genetic linkage mapping is that nonpolymorphic as well as polymorphic DNA markers can be ordered at a very high level of resolution. Although RH mapping is a statistical rather than a physical mapping method, the frequency of X-ray breakage between two markers has been found to be directly related to the physical distance between them, such that at a dose of 8000 rads of X rays, 1% breakage between markers corresponds to a physical distance of approximately 50 kb (Cox *et al.*, 1990; Burmeister *et al.*, 1991).

Several different mathematical models and methods for the statistical analysis of RH mapping data have been described, each with its own strengths and weaknesses (Cox *et al.*, 1990; Boehnke *et al.*, 1991; Falk, 1991;

[1] To whom correspondence should be addressed at the University of California, 401 Parnassus Avenue, P.O. Box 0984, San Francisco, CA 94143-0984.

0888-7543/92 $5.00

Lawrence *et al.*, 1991; Bishop and Crockford, 1992; Chakravarti and Reefer, 1992; Green, 1992). However, for the limited number of data sets analyzed to date, no single model or method of analysis has been shown to be clearly preferred in all cases. Models that assume a single retention frequency for all markers in a set of radiation hybrids are attractive, since they provide mathematically simple means for estimating the distance between markers as well as the likelihood of one map order versus another. However, for those data sets in which the retention of different markers is clearly not identical, it is not known whether the use of a single retention frequency model will lead to incorrect maps.

In this report we use two different mathematical models for analyzing RH data: the equal retention model, which assumes a single retention frequency for all markers in the radiation hybrids, and the unequal retention model, which permits a different retention frequency for each marker. In addition, we use two different statistical estimation procedures to analyze the data: the method of moments and maximum likelihood analysis. Despite the fact that the marker retention is not identical for the different markers in this data set, the use of the equal retention model and the method of moments results in a framework map of 8 markers ordered at 1000:1 odds that is the same as that obtained using the unequal retention model and the method of moments. Analysis of this data set using the equal retention model and a maximum likelihood estimation approach yields the same framework map as the method of moments estimation procedure. In addition, the maximum likelihood approach results in a comprehensive map that gives the most likely order for all 16 distinguishable loci. Our RH map assigns new markers to the NF2 region and provides additional order and distance information for markers previously localized to this segment of human chromosome 22.

MATERIALS AND METHODS

DNA probes. The chromosome 22 DNA marker loci used in this study, with the probe that recognizes each locus listed in parentheses following that locus, were D22S33 (pH4), D22S36 (pH11), D22S37 (pH13), D22S41 (pH20), D22S42 (pH22), D22S44 (pH35), D22S46 (pH43), D22S47 (pH59), D22S48 (pH60), and D22S56 (pH97b). These probes were isolated from a flow-sorted library (LL22NS01) constructed at the Biomedical Sciences Division, Lawrence Livermore National Laboratory (Livermore, CA) (Budarf *et al.*, 1991). DNA marker D22S28 (W23C) was isolated from the same library described above (Rouleau *et al.*, 1989). The following genes and anonymous markers were also used: platelet-derived growth factor β polypeptide chain gene, PDGFB (pA-csis) (gift from Dan Mirda); myoglobin gene, MB (pHM27.B2.9) (Weller *et al.*, 1984); leukemia inhibitory factor gene, LIF (pC4.7) (Lowe *et al.*, 1989); D22S1 (pMS3-18) (Barker *et al.*, 1984); and D22S15 (DP22) (Rouleau *et al.*, 1988). The breakpoint cluster region gene (BCR) and a BCR-like locus (BCRL2), each of which maps to a distinct region of 22q11, were detected with a single probe derived from the 3′ end of a BCR cDNA clone (Croce *et al.*, 1987; Budarf *et al.*, 1988).

Cell lines and culture conditions. Cell line EYEF3A6 (GM10027) is a Chinese hamster-human hybrid cell line containing an intact human chromosome 22 and fragments of human chromosomes 15 and 19 (Van Keuren *et al.*, 1987; Ledbetter *et al.*, 1990). EYEF3A6 cells were grown in Ham's F12 medium supplemented with 10% dialyzed fetal calf serum (FCS), penicillin, and streptomycin. 380-6, a hypoxanthine–guanine phosphoribosyltransferase (HPRT)-deficient hamster cell line, was cultured in Dulbecco's modified Eagle's medium (DMEM) containing 10% FCS, penicillin, and streptomycin.

Production of radiation hybrids. X-irradiation and cell fusion were performed as previously described (Cox *et al.*, 1989). Briefly, EYEF3A6 cells were irradiated with 8000 rads of X rays and fused in a 1:1 ratio with nonirradiated HPRT-deficient 380-6 hamster cells by polyethylene glycol. The fused cells were then cultured in HAT medium (DMEM plus 100 μM hypoxanthine, 1 μM aminopterin, and 12 μM thymidine) to eliminate the nonhybrid 380-6 cells and to select for hybrids retaining the hamster HPRT gene from the irradiated EYEF3A6 cells. Two to three weeks after fusion, an average of one EYEF3A6 × 380-6 radiation hybrid clone per plate was observed, indicating a hybrid formation efficiency of approximately one hybrid per 1.5×10^6 recipient 380-6 cells. No colonies formed from either 10^7 irradiated, nonfused EYEF3A6 cells or 10^7 unfused 380-6 cells grown in HAT medium. A total of 130 independent colonies that grew under HAT selection were expanded in HAT medium. DNA was isolated from 86 of the fastest growing hybrids and was analyzed for the retention of human chromosome 22 DNA markers by Southern blot analysis as described below. Southern blot data from one of the 86 hybrids were not included in the statistical analysis due to inconsistent results for multiple markers on different blots; thus the map is based on results using 85 radiation hybrids. In addition, it should be noted that not all hybrids could be scored reliably for all markers, resulting in some missing data (see Tables 1 and 2).

Southern blot analysis and hybridization. Genomic DNA was isolated from cultured cells as previously described (Cox *et al.*, 1990), digested to completion with *Hin*dIII, electrophoresed through 1% agarose gels, and transferred to Hybond N plus nylon filters (Amersham). The Southern transfers were prehybridized, hybridized with radiolabeled inserts, washed, and stripped of probe prior to rehybridization, according to the manufacturer's recommendations. Probes were radioactively labeled with [α^{32}P]dCTP by the random primer procedure (Feinberg and Vogelstein, 1984). The hybridized filters were exposed to X-ray film with an intensifying screen at −70°C for 3–7 days.

Analysis of radiation hybrid data using the method of moments. We analyzed the RH data using the method of moments, as previously described (Cox *et al.*, 1990). In the N-locus case, the likelihood of the RH data is a function of $N - 1$ breakage probabilities between adjacent loci, and one or more retention probabilities. The general model allows all $N(N + 1)/2$ such retention probabilities to differ (Cox *et al.*, 1990). Here we also consider an equal retention probability model, in which all retention probabilities are assumed equal. This model has the advantage of requiring fewer parameters than the general, unequal retention frequency model and is computationally much simpler. Computation of the likelihood for the equal retention model scales linearly with the number of loci N, while computation for the unequal retention model scales geometrically with N (Boehnke *et al.*, 1991). Both the equal and the unequal retention models assume that breakage occurs at random positions along the chromosome and that fragments are retained independently. Using the method of moments, we estimate the frequency of breakage between two markers, A and B, by the equation

$$\theta = \{(A^+B^-) + (A^-B^+)\}/\{(T)[R_A + R_B - (2)(R_A)(R_B)]\},$$

where (A^+B^-) is the observed number of hybrid clones retaining marker A but not marker B, (A^-B^+) is the observed number of hybrid clones retaining marker B but not marker A, T is the total number of hybrids analyzed for both markers A and B, R_A is the fraction of all hybrids analyzed for marker A that retain marker A, and R_B is the fraction of all hybrids analyzed for marker B that retain marker B. For the equal retention model, the single retention frequency R is calculated as

$$R = \sum_{M=1}^{N} R_M / \sum_{M=1}^{N} T_M,$$

where R_M is defined as the number of hybrids that retain marker M, T_M is defined as the total number of hybrids scored for marker M, and N is defined as the total number of markers. The mapping function, $D = -\ln(1 - \theta)$, is used to estimate D, the distance between two markers. D is expressed in centirays. It is important to include information about X-ray dose when describing the centiray distance between two markers, since the frequency of breakage, and thus D, depends on the amount of radiation used to generate the radiation hybrids. A distance of 1 cR_{8000} between two markers corresponds to a 1% frequency of breakage between the markers after exposure to 8000 rads of X rays.

The lod score for a marker pair is defined as

$$\text{lod}(\theta) = \log[L(\theta)/L(\theta = 1)],$$

where $L(\theta)$ is the likelihood of obtaining the observed data for a given pair of markers and $L(\theta = 1)$ is the likelihood assuming that the two markers are not linked; that is, $\theta = 1$. This lod score can be used to identify marker pairs that are significantly linked, in a manner analogous to meiotic mapping (Cox *et al.*, 1990).

In principle, we can use the method of moments to determine the order of markers with the highest overall likelihood given the data. However, for maps consisting of more than four loci, it is impractical to use the unequal retention model and the method of moments to calculate the likelihood for even a single order including all loci (Cox *et al.*, 1990). In contrast, using the equal retention model and the method of moments and assuming that all hybrids are scored for all markers (i.e., no missing data), the overall likelihood for a particular order of many loci can be easily determined by summing the individual two-point likelihoods calculated using adjacent loci. Unfortunately, our chromosome 22 data set has missing data, so we cannot use this approach to determine the overall likelihood of a particular order of many loci. Therefore, we have used the method of moments considering groups of four loci at a time to construct a "framework map" of loci ordered at odds of 1000 to 1 (Cox *et al.*, 1990). In contrast to the maximum likelihood analysis described below, this method includes only those hybrids that have been scored for all four markers in each group, and thus does not include incomplete data. For a given set of four markers, each of the 12 possible orders with likelihoods greater than one thousandth of the most likely order for these four markers is used to construct the map. Such orders for different groups of four markers are used to build a consistent map that includes as many markers as possible. To identify those groups of four markers most useful for constructing the framework map, we first used two-point distances to build a map including all markers, such that the distance between adjacent markers is minimized (Cox *et al.*, 1990). This map is used to select groups of four markers that are considered initially in the construction of the framework map.

Nonframework markers are positioned on the framework map as follows. A nonframework locus is placed sequentially in each of the intervals defined by a set of three framework markers, and the likelihood for each of these locus orders is determined. Those orders with likelihoods greater than one thousandth of the most likely order for the set of four markers represent possible locations for the nonframework locus on the framework map. Likelihood ratios are used to determine the relative odds that a nonframework locus maps within one framework map interval versus another.

Analysis of radiation hybrid data using a maximum likelihood approach. In addition to the method of moments described above, we analyzed the data using the equal retention model and a multipoint maximum likelihood method (Boehnke *et al.*, 1991). Unlike the method of moments, this maximum likelihood method makes use of data on all loci simultaneously, including information on partially typed hybrids. For a given locus order, breakage and retention probabilities are estimated by those values that maximize the likelihood for the RH mapping data. Orders can be compared by their maximum likelihoods, the order with the largest maximum likelihood being best supported by the data.

Since it is not practical to consider explicitly all possible locus orders, we used a stepwise locus-ordering algorithm to identify the most likely locus order (Boehnke *et al.*, 1991). This algorithm builds locus orders by adding one locus at a time. At each stage, it keeps under consideration those partial locus orders no more than K times less likely than the current best partial locus order. Analogous methods are often employed in constructing genetic linkage maps (Barker *et al.*, 1987). We carried out stepwise locus ordering for the equal retention model for the 16 distinguishable loci with $K = 10^3$.

Stepwise locus ordering results in a list of the locus orders with the largest maximum likelihoods. The comprehensive map is defined as the order from this list with the highest maximum likelihood. A framework map is constructed using orders from this list that have maximum likelihoods no less than one thousandth that of the comprehensive map. We define framework loci as a set of loci whose positions are consistent relative to one another among these orders. As there is no simple algorithm for constructing the largest set of framework loci, this is done by eye. The remaining loci are then considered one at a time to see if any can be added with 1000:1 support to a specific position on the map. Nonframework markers are positioned on the framework map as described above. Each locus is placed sequentially in each of the map intervals defined by the framework markers, and the maximum likelihood for each of these locus orders is determined. Those orders with likelihoods greater than one thousandth of the most likely order represent possible locations for the nonframework locus on the framework map. Likelihood ratios are used to determine the relative odds that a nonframework locus maps within one possible framework interval versus another.

RESULTS

Radiation Hybrid Data

To construct an RH map of the NF2 region on human chromosome 22, we isolated DNA from 85 independent radiation hybrids and used Southern blot analysis to determine the presence or absence of 18 human chromosome 22-specific loci in each DNA sample (see Materials and Methods). Although in a few cases the human probes cross-hybridized with hamster DNA, the human-specific bands could always be distinguished from the hamster bands on the basis of size. The retention frequency of the individual human loci in the radiation hybrids, defined as the fraction of hybrids scored for a locus that retain that locus, ranged from 17 to 42% (Table 1). The segregation patterns observed for all possible pairs of loci in the radiation hybrids are shown in Table 2.

Analysis of Radiation Hybrid Data Using the Method of Moments

We initially compared the equal and the unequal retention models using the method of moments to estimate the frequency of breakage, θ, and to calculate the lod score for each pair of markers. The distance between two markers, D, is expressed in cR_{8000} (see Materials and Methods). As shown in Table 2, the estimates of distance and lod score are very similar using both the equal and the unequal retention model, despite the fact that the retention frequency is not the same for all of the markers in this data set. Three of the markers, D22S41, D22S42, and D22S46, co-segregated in all of the radiation hybrids, with no evidence of breakage between them

TABLE 1

Retention Frequencies

Locus	No. of hybrids scored	Retention frequency
D22S36	80	0.24
BCRL2	71	0.42
BCR	71	0.34
D22S1	83	0.30
D22S33	70	0.39
D22S41	84	0.32
D22S42	84	0.31
D22S46	85	0.32
D22S56	85	0.27
LIF	84	0.18
D22S37	85	0.21
D22S15	83	0.17
D22S44	83	0.20
D22S47	84	0.18
D22S28	82	0.17
D22S48	85	0.19
MB	84	0.17
PDGFB	85	0.20

Note. The human chromosome 22 loci scored in the radiation hybrids, the total number of hybrids scored for each locus, and the proportion of hybrids scored for each locus that retain that locus (Retention frequency) are listed.

(Table 2). Therefore, we used only one of these three loci, D22S41, in subsequent analyses. Since it was impractical to calculate the overall likelihood for even a single order of the 16 distinguishable loci under either the unequal retention model or the equal retention model using the method of moments, we constructed a framework map of loci ordered with odds of 1000:1 by considering groups of four markers at a time (see Materials and Methods). As a first step in the construction of this framework map, we used a trial and error process and two-point distance information from Table 2 to construct a map that includes the entire set of 16 markers in an order such that the sum of the distances between adjacent markers is minimized. Under the equal retention model, this map consists of the marker order D22S36–BCR2L–BCR–D22S1–D22S33–D22S41–D22S56–LIF–D22S37–D22S44–D22S15–D22S28–D22S47–D22S48–MB–PDGFB, spanning a distance of 307 cR_{8000}. Under the unequal retention model, the map spans a distance of 301 cR_{8000} with the same order as above, except that the loci D22S33 and D22S1 are inverted. These maps were used to select groups of markers for four-point likelihood calculations. Under the equal retention model, the likelihood for the order BCR2L–BCR–D22S1–D22S56 is more than 1000 times greater than the likelihood of any of the other 11 possible orders of these four markers (Table 3). Similarly, the likelihoods of the orders BCR–D22S1–D22S56–D22S37,D22S1–D22S56–D22S37–D22S15 and D22S56–D22S37–D22S15–D22S28 are more than 1000 times the likelihood of each alternative order, respectively (Table 3). Taken together, this set of four four-point orders is consistent with the unique framework order BCR2L–BCR–D22S1–D22S56–D22S37–D22S15–D22S28. Similar analyses place PDGFB distal to D22S28 at the opposite end of the map from BCR2L (data not shown). Using the approach described under Materials and Methods, each of the remaining 8 nonframework loci can be localized to a region of the framework map consisting of two adjoining intervals with greater than 1000:1 odds (Fig. 1A). Similar analyses assuming an unequal retention frequency model result in a framework map identical to that described above, and relative likelihoods for the position of nonframework markers that are very similar to those obtained using the equal retention frequency model (data not shown).

Maximum Likelihood Multipoint Analysis of the Radiation Hybrid Data

As shown above, data analysis using the method of moments provides a single framework map of 8 markers ordered at an odds of 1000:1 employing either the equal retention model or the unequal retention model. However, given the missing data in our data set, it is not practical to use the method of moments to calculate overall likelihoods for maps including all 16 distinguishable markers (see Materials and Methods). Furthermore, since each four-point analysis using the method of moments includes only those hybrids scored for all 4 markers, this method does not include all of the available data, which reduces the power of the analysis. In light of these considerations, we analyzed the data using a maximum likelihood approach, which provides overall likelihoods for maps of the 16 distinguishable markers and incorporates all of the data (see Materials and Methods). We began the maximum likelihood multipoint analysis by carrying out stepwise locus ordering. Table 4 presents the 36 locus orders with maximum likelihoods no more than 1000 times less than that of the best locus order under the equal retention probability model. The most likely comprehensive map spans a distance of 302 cR_{8000} (Fig. 1B). The framework map constructed using the maximum likelihood approach (see Materials and Methods) is identical to that obtained using the method of moments, despite the fact that the method of moments analysis does not incorporate all the data. In addition, the relative likelihoods for the positions of nonframework loci are very similar, although not identical, using the two different methods of analysis (Figs. 1A and 1C).

DISCUSSION

We have constructed an RH map of human chromosome 22 with 18 22q11.1–22q13.1 markers, 16 of which are distinguishable by X-ray breakage in radiation hybrids. Eight of these markers are uniquely ordered on a framework map with greater than 1000:1 odds, while the remaining nonframework markers are all localized to regions consisting of two adjoining intervals on the framework map with greater than 1000:1 odds. On the basis of

TABLE 2

Segregration Patterns

MARKERS		# OF CLONES OBSERVED					UNEQUAL RETENTION			EQUAL RETENTION		
A	B	++	+-	-+	--	TOT	LOD	θ	cR_{8000}	LOD	θ	cR_{8000}
D22S36	BCR2L	19	0	6	41	66	10.60	0.20	22	10.09	0.24	28
D22S36	BCR	13	6	8	40	67	3.73	0.50	70	3.61	0.56	81
D22S36	D22S1	9	10	11	48	78	1.36	0.68	114	1.25	0.72	126
D22S36	D22S33	10	5	12	38	65	2.07	0.59	90	1.73	0.70	119
D22S36	D22S41	10	9	12	48	79	1.68	0.65	106	1.52	0.71	123
D22S36	D22S46	10	9	12	49	80	1.73	0.65	105	1.56	0.70	120
D22S36	D22S42	9	9	12	49	79	1.47	0.66	109	1.29	0.71	123
D22S36	D22S56	10	9	9	52	80	2.32	0.59	90	2.26	0.60	91
D22S36	LIF	8	11	4	56	79	2.41	0.57	85	2.43	0.51	70
D22S36	D22S37	10	9	5	56	80	3.47	0.50	70	3.50	0.47	63
D22S36	D22S44	8	11	7	52	78	1.59	0.67	111	1.60	0.61	95
D22S36	D22S15	9	10	3	56	78	3.37	0.51	72	3.39	0.44	59
D22S36	D22S28	7	12	5	54	78	1.54	0.67	110	1.53	0.58	87
D22S36	D22S47	6	13	6	54	79	0.93	0.73	129	0.89	0.64	102
D22S36	D22S48	6	13	7	54	80	0.80	0.74	136	0.76	0.67	109
D22S36	MB	6	13	5	55	79	1.10	0.70	121	1.07	0.61	93
D22S36	PDGFB	9	10	6	55	80	2.49	0.58	88	2.51	0.53	76
BCR2L	BCR	18	9	4	36	67	5.21	0.41	53	5.60	0.52	73
BCR2L	D22S1	17	13	5	35	70	3.33	0.55	79	3.47	0.68	115
BCR2L	D22S33	18	7	7	29	61	3.81	0.48	65	4.58	0.61	94
BCR2L	D22S41	18	12	6	35	71	3.50	0.54	77	3.80	0.67	112
BCR2L	D22S46	18	12	6	35	71	3.52	0.54	77	3.80	0.67	112
BCR2L	D22S42	17	12	6	35	70	3.29	0.55	79	3.47	0.68	115
BCR2L	D22S56	16	14	5	36	71	3.07	0.58	86	2.95	0.71	125
BCR2L	LIF	12	18	2	39	71	2.62	0.63	98	1.77	0.75	139
BCR2L	D22S37	13	17	3	38	71	2.54	0.62	96	1.98	0.75	139
BCR2L	D22S44	10	20	4	37	71	1.07	0.74	136	0.57	0.90	230
BCR2L	D22S15	11	19	2	38	70	2.14	0.67	110	1.28	0.80	160
BCR2L	D22S28	9	19	3	38	69	1.35	0.71	124	0.71	0.85	189
BCR2L	D22S47	10	20	3	38	71	1.42	0.72	127	0.76	0.86	198
BCR2L	D22S48	10	20	4	37	71	1.16	0.75	138	0.57	0.90	230
BCR2L	MB	9	21	3	37	70	1.06	0.76	145	0.42	0.91	244
BCR2L	PDGFB	11	19	3	38	71	1.68	0.68	115	1.11	0.82	174
BCR	D22S1	18	5	4	43	70	7.77	0.30	35	8.02	0.34	42
BCR	D22S33	19	3	5	32	59	7.20	0.29	35	7.97	0.36	45
BCR	D22S41	19	5	5	42	71	7.49	0.32	38	7.90	0.37	47
BCR	D22S46	19	5	5	42	71	7.50	0.32	38	7.90	0.37	47
BCR	D22S42	18	5	5	42	70	7.12	0.33	39	7.43	0.38	48
BCR	D22S56	15	9	5	42	71	4.48	0.46	62	4.53	0.52	74
BCR	LIF	9	15	5	42	71	1.48	0.71	124	1.15	0.75	139
BCR	D22S37	11	13	5	42	71	2.28	0.62	98	2.05	0.67	112
BCR	D22S44	9	14	5	42	70	1.52	0.67	111	1.30	0.72	128
BCR	D22S15	9	15	4	42	70	1.71	0.69	118	1.30	0.72	128
BCR	D22S28	8	16	5	42	71	1.09	0.75	139	0.78	0.79	155
BCR	D22S47	7	17	5	42	71	0.69	0.78	153	0.48	0.82	174
BCR	D22S48	9	15	4	43	71	1.63	0.67	111	1.34	0.71	125
BCR	MB	9	15	3	43	70	1.94	0.66	107	1.51	0.68	115
BCR	PDGFB	10	14	4	43	71	2.07	0.63	99	1.80	0.67	112
D22S1	D22S33	24	0	2	43	69	16.00	0.06	7	16.60	0.08	8
D22S1	D22S41	24	1	1	56	82	17.91	0.06	6	18.15	0.06	7
D22S1	D22S46	24	1	1	57	83	18.06	0.06	6	18.26	0.06	7
D22S1	D22S42	23	1	1	57	82	17.56	0.06	6	17.68	0.06	7
D22S1	D22S56	20	5	1	57	83	12.28	0.18	19	12.29	0.19	21
D22S1	LIF	14	11	1	57	83	6.46	0.39	49	6.00	0.38	49
D22S1	D22S37	15	10	2	56	83	6.61	0.38	47	6.37	0.38	49
D22S1	D22S44	13	11	3	54	81	4.84	0.45	60	4.60	0.46	62
D22S1	D22S15	11	13	3	55	82	3.66	0.53	75	3.26	0.52	73
D22S1	D22S28	11	12	2	55	80	4.24	0.47	64	3.84	0.47	63
D22S1	D22S47	12	13	2	55	82	4.31	0.49	68	3.94	0.49	67
D22S1	D22S48	14	11	1	57	83	6.38	0.38	49	6.00	0.38	49
D22S1	MB	12	12	1	57	82	5.21	0.43	56	4.73	0.42	55
D22S1	PDGFB	12	13	4	54	83	3.54	0.54	77	3.32	0.55	79
D22S33	D22S41	25	2	0	42	69	16.15	0.06	7	17.06	0.08	8
D22S33	D22S46	25	2	0	43	70	16.34	0.06	6	17.18	0.08	8

TABLE 2—*Continued*

MARKERS		# OF CLONES OBSERVED					UNEQUAL RETENTION			EQUAL RETENTION		
A	B	++	+−	−+	−−	TOT	LOD	θ	cR_{8000}	LOD	θ	cR_{8000}
D22S33	D22S42	24	2	0	43	69	15.94	0.06	7	16.60	0.08	8
D22S33	D22S56	21	6	0	43	70	11.21	0.19	21	11.35	0.23	26
D22S33	LIF	14	13	0	43	70	5.46	0.44	57	4.54	0.49	68
D22S33	D22S37	15	12	1	42	70	5.40	0.43	56	4.87	0.49	68
D22S33	D22S44	13	13	2	40	68	3.83	0.51	71	3.32	0.59	88
D22S33	D22S15	11	15	2	41	69	2.97	0.58	87	2.21	0.66	107
D22S33	D22S28	11	14	1	41	67	3.46	0.53	75	2.67	0.60	91
D22S33	D22S47	12	15	1	41	69	3.50	0.54	78	2.77	0.62	96
D22S33	D22S48	13	14	1	42	70	4.16	0.50	69	3.46	0.57	84
D22S33	MB	11	15	1	42	69	3.31	0.55	79	2.49	0.62	96
D22S33	PDGFB	12	15	4	39	70	2.46	0.63	99	1.97	0.72	128
D22S41	D22S46	27	0	0	57	84	22.91	0	0	23.37	0	0
D22S41	D22S42	26	0	0	57	83	22.42	0	0	22.77	0	0
D22S41	D22S56	23	4	0	57	84	15.49	0.11	12	15.58	0.13	14
D22S41	LIF	15	11	0	57	83	7.54	0.34	42	6.89	0.35	44
D22S41	D22S37	17	10	1	56	84	8.10	0.33	40	7.74	0.35	43
D22S41	D22S44	15	11	2	55	83	6.27	0.40	51	5.89	0.42	54
D22S41	D22S15	12	13	2	55	82	4.52	0.48	65	3.94	0.49	67
D22S41	D22S28	13	12	1	55	81	5.64	0.42	54	5.02	0.43	56
D22S41	D22S47	14	13	1	56	84	5.74	0.43	57	5.17	0.44	59
D22S41	D22S48	15	12	1	56	84	6.49	0.40	51	5.97	0.41	53
D22S41	MB	13	13	1	56	83	5.40	0.44	58	4.74	0.45	60
D22S41	PDGFB	13	14	4	53	84	3.68	0.55	79	3.37	0.57	84
D22S46	D22S42	26	0	0	58	84	22.58	0	0	22.89	0	0
D22S46	D22S56	23	4	0	58	85	15.62	0.11	12	15.69	0.13	13
D22S46	LIF	15	11	0	58	84	7.60	0.34	42	6.97	0.35	43
D22S46	D22S37	17	10	1	57	85	8.18	0.33	40	7.83	0.34	42
D22S46	D22S44	15	11	2	55	83	6.25	0.40	51	5.89	0.42	54
D22S46	D22S15	12	13	2	56	83	4.56	0.48	65	4.01	0.48	66
D22S46	D22S28	13	12	1	56	82	5.70	0.42	54	5.09	0.42	55
D22S46	D22S47	14	13	1	56	84	5.72	0.44	57	5.17	0.44	59
D22S46	D22S48	15	12	1	57	85	6.55	0.40	50	6.05	0.41	52
D22S46	MB	13	13	1	57	84	5.45	0.44	58	4.81	0.44	59
D22S46	PDGFB	13	14	4	54	85	3.73	0.54	78	3.43	0.56	83
D22S42	D22S56	22	4	0	58	84	15.09	0.12	12	15.13	0.13	14
D22S42	LIF	14	11	0	58	83	7.04	0.35	43	6.51	0.35	44
D22S42	D22S37	16	10	1	57	84	7.66	0.34	41	7.36	0.35	43
D22S42	D22S44	14	11	2	55	82	5.76	0.41	53	5.45	0.42	55
D22S42	D22S15	11	13	2	56	82	4.08	0.49	67	3.61	0.49	67
D22S42	D22S28	12	12	1	56	81	5.17	0.43	56	4.66	0.43	56
D22S42	D22S47	13	13	1	56	83	5.20	0.45	59	4.74	0.45	60
D22S42	D22S48	14	12	1	57	84	6.03	0.41	52	5.61	0.41	53
D22S42	MB	12	13	1	57	83	4.92	0.45	60	4.39	0.45	60
D22S42	PDGFB	12	14	4	54	84	3.32	0.56	81	3.07	0.57	84
D22S56	LIF	15	7	0	62	84	9.75	0.24	27	9.48	0.22	25
D22S56	D22S37	17	6	1	61	85	10.55	0.22	25	10.42	0.22	25
D22S56	D22S44	15	8	2	58	83	7.58	0.33	40	7.44	0.32	39
D22S56	D22S15	12	9	2	60	83	5.98	0.38	48	5.74	0.35	44
D22S56	D22S28	12	9	2	59	82	5.89	0.38	49	5.66	0.36	44
D22S56	D22S47	13	10	2	59	84	5.94	0.41	52	5.71	0.38	48
D22S56	D22S48	14	9	2	60	85	6.87	0.36	45	6.67	0.34	42
D22S56	MB	12	10	2	60	84	5.59	0.41	53	5.33	0.38	48
D22S56	PDGFB	11	12	6	56	85	2.92	0.58	88	2.82	0.56	83
LIF	D22S37	14	1	3	66	84	11.28	0.15	16	11.56	0.13	14
LIF	D22S44	12	3	4	63	82	7.74	0.28	32	8.02	0.23	26
LIF	D22S15	11	3	3	66	83	7.85	0.25	29	8.43	0.19	21
LIF	D22S28	10	4	3	64	81	6.53	0.30	36	7.09	0.23	26
LIF	D22S47	10	5	4	64	83	5.59	0.37	46	6.03	0.29	34
LIF	D22S48	10	5	5	64	84	5.19	0.40	51	5.56	0.32	38
LIF	MB	9	5	4	65	83	5.07	0.38	48	5.62	0.29	34
LIF	PDGFB	9	6	7	62	84	3.55	0.50	70	3.79	0.41	53
D22S37	D22S44	15	3	2	63	83	10.84	0.18	20	10.98	0.16	17
D22S37	D22S15	13	3	1	66	83	10.66	0.16	17	11.01	0.13	14
D22S37	D22S28	11	6	3	62	82	6.12	0.35	44	6.34	0.29	35

TABLE 2—*Continued*

MARKERS		# OF CLONES OBSERVED					UNEQUAL RETENTION			EQUAL RETENTION		
A	B	++	+−	−+	−−	TOT	LOD	θ	cR_{8000}	LOD	θ	cR_{8000}
D22S37	D22S47	11	7	4	62	84	5.27	0.42	54	5.44	0.35	43
D22S37	D22S48	12	6	4	63	85	6.26	0.37	46	6.43	0.31	38
D22S37	MB	11	6	3	64	84	6.26	0.35	43	6.52	0.29	34
D22S37	PDGFB	10	8	7	60	85	3.36	0.54	78	3.46	0.47	63
D22S44	D22S15	13	2	1	65	81	11.4	0.12	13	11.80	0.10	10
D22S44	D22S28	12	4	2	62	80	8.28	0.25	28	8.56	0.20	22
D22S44	D22S47	12	5	3	63	83	7.21	0.31	37	7.45	0.26	30
D22S44	D22S48	13	4	3	63	83	8.33	0.27	31	8.54	0.22	25
D22S44	MB	12	4	2	64	82	8.43	0.24	28	8.76	0.19	22
D22S44	PDGFB	11	6	5	61	83	5.18	0.41	53	5.36	0.35	44
D22S15	D22S28	10	3	2	65	80	7.74	0.22	25	8.48	0.17	18
D22S15	D22S47	10	4	3	65	82	6.60	0.30	35	7.18	0.23	26
D22S15	D22S48	10	4	4	65	83	6.13	0.33	40	6.63	0.26	30
D22S15	MB	10	4	3	66	83	6.63	0.30	36	7.28	0.22	25
D22S15	PDGFB	9	5	7	62	83	3.87	0.48	65	4.14	0.38	49
D22S28	D22S47	13	1	0	67	81	13.66	0.04	4	14.34	0.03	3
D22S28	D22S48	13	1	1	67	82	12.48	0.08	9	13.07	0.06	7
D22S28	MB	12	1	1	67	81	11.72	0.09	9	12.50	0.07	7
D22S28	PDGFB	10	4	6	62	82	5.11	0.40	52	5.40	0.32	39
D22S47	D22S48	14	1	2	67	84	12.18	0.12	13	12.59	0.10	10
D22S47	MB	12	2	2	67	83	9.94	0.17	18	10.56	0.13	14
D22S47	PDGFB	10	5	7	62	84	4.37	0.47	63	4.59	0.38	48
D22S48	MB	14	1	0	69	84	14.58	0.04	4	15.18	0.03	3
D22S48	PDGFB	11	5	6	63	85	5.30	0.41	53	5.52	0.34	42
MB	PDGFB	11	3	6	64	84	6.22	0.36	44	6.52	0.29	34

Note. All pairwise combinations of the 18 chromosome 22 DNA markers used to generate the radiation hybrid map are listed. For each marker pair, the number of radiation hybrids containing both markers A and B (++), containing marker A but not B (+−), containing marker B but not A (−+), and containing neither marker A nor B (−−), as well as the total number of hybrids analyzed for both markers (TOT), are listed. The lod scores (LOD), breakage probability estimates (θ), and distance estimates (cR_{8000}) in RH map units were calculated using the method of moments with either the unequal retention probability model (Unequal retention) or the equal retention probability model (Equal retention) (see Materials and Methods).

our RH map, the NF2 region of chromosome 22, between D22S1 and D22S28, is the most likely location for 9 of the 18 markers studied: D22S33, D22S41, D22S42, D22S46, D22S56, LIF, D22S37, D22S44, and D22S15.

We have used two different statistical estimation procedures to analyze our data: the method of moments and a maximum likelihood approach. The method of moments provides a simple, rapid approach for constructing RH maps, particularly in those cases where an equal retention frequency model can be employed. In such cases, an overall likelihood for a particular order of markers can be obtained by simply summing the lod scores for adjacent loci (Richard *et al.*, 1991). However, it is important to recognize that summing lod scores for adjacent locus pairs to obtain the multipoint maximum lod score requires that every locus be typed in every hybrid. In cases where there are substantial missing data, as is the case for the data set analyzed here, such an approach should not be employed. In such situations, one can still use the method of moments to calculate likelihoods, considering four loci at a time. However, in such cases, the approach no longer provides a practical means for determining the overall likelihood of a given order of more than four markers, and does not incorporate information from partially typed hybrids in the analysis. In contrast, the maximum likelihood approach does incorporate information from partially typed hybrids in the calculation of overall likelihoods, making it

TABLE 3

Four-Point Analysis Using the Method of Moments

Most likely order	Second most likely order	Odds
BCR2L–BCR–D22S1–D22S56	BCR–D22S1–D22S56–BCR2L	1.7×10^3
BCR–D22S1–D22S56–D22S37	BCR–D22S1–D22S37–D22S56	9.2×10^6
D22S1–D22S56–D22S37–D22S15	D22S1–D22S56–D22S15–D22S37	7.0×10^3
D22S56–D22S37–D22S15–D22S28	D22S15–D22S37–D22S56–D22S28	5.6×10^3

Note. An equal retention probability model and the method of moments were used to estimate the likelihoods of the 12 possible orders for each set of 4 markers listed above. The most likely order and the second most likely order, as well as the odds favoring the most likely order over the second most likely order, are listed for each of the 4 sets of markers. The odds were determined by likelihood ratios (see Materials and Methods).

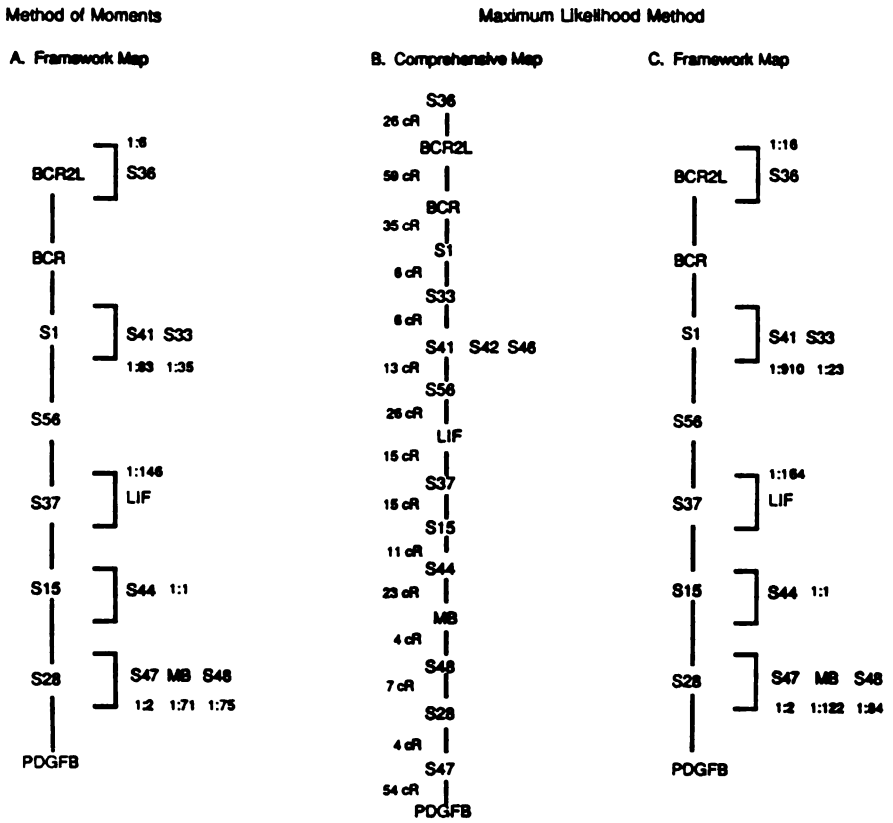

FIG. 1. (A and C) Framework RH maps constructed assuming an equal retention frequency model using the method of moments analysis and the maximum likelihood analysis, respectively. Brackets mark the regions in which loci not in the framework map cannot be excluded based on relative maximum likelihoods of 1000:1. Numbers adjacent to a locus provide relative likelihoods for the two possible positions of that locus; numbers above (below) a locus indicate that the upper (lower) position has the larger maximum likelihood. For example, LIF is 164 times more likely to be located between S56 and S37 than between S37 and S15 on the maximum likelihood framework map. (B) The most likely comprehensive RH map based on the maximum likelihood method. Distances between the markers are indicated in cR_{5000} to the left of the diagrams. The DNA markers are abbreviated by deleting D22, so that D22S1 = S1.

possible to compare the likelihoods for different maps and to identify the map that best fits the data. The only disadvantage of the maximum likelihood method is that it is more mathematically complex than the method of moments and requires a sophisticated computer software package. In contrast, the mathematical simplicity of the method of moments makes this approach more attractive for initial interactive data analysis by the experimental scientist.

In the present case, the order of markers on the framework map, as well as the likelihoods for the positions of the nonframework markers on this framework map, obtained with the method of moments is very similar to that obtained with the maximum likelihood approach. The most striking exception is the placement of marker D22S41, which is placed in the interval D22S1–D22S56 versus the interval BCR–D22S1 with odds of 910:1 using maximum likelihood analysis, but with odds of only 83:1 using the method of moments. Although the method of moments and the maximum likelihood analysis give similar results for this data set, we recommend the maximum likelihood approach in those cases where there are significant missing data.

Recent studies have demonstrated that it is much easier to score for the presence of human DNA markers in radiation hybrids by using PCR-based assays and analyzing ethidium-stained gels than by using Southern blotting procedures (Richard *et al.*, 1991). This change in methodology is likely to produce data sets with many fewer missing data than has been the case to date. Given such data sets with little or no missing data and assuming an equal retention frequency model, the method of moments approach can be expected to give results very similar to those obtained using the computationally more complex maximum likelihood approach. Whether the mathematical simplicity of the method of moments will make it the preferred method of analysis in such cases will require further study.

Irrespective of the statistical estimation procedure employed, analysis of RH data is significantly less com-

TABLE 4

Maximum Likelihood Locus Orders for the Chromosome 22 Radiation Hybrid Mapping Data

Rank	Locus Order	Relative Likelihood
1	S36 BCR2L BCR S1 S33 S41 S56 LIF S37 S15 S44 MB S48 S28 S47 PDGFB	1
2	S36 BCR2L BCR S1 S33 S41 S56 LIF S37 S15 S44 S47 S28 S48 MB PDGFB	3
3	S36 BCR2L BCR S1 S33 S41 S56 LIF S37 S44 S15 S47 S28 S48 MB PDGFB	5
4	S36 BCR2L BCR S1 S33 S41 S56 LIF S37 S15 S44 MB S48 S47 S28 PDGFB	6
5	S36 BCR2L BCR S1 S33 S41 S56 LIF S37 S15 S44 S28 S47 S48 MB PDGFB	8
6	S36 BCR2L BCR S1 S33 S41 S56 LIF S37 S44 S15 S28 S47 S48 MB PDGFB	12
7	BCR2L S36 BCR S1 S33 S41 S56 LIF S37 S15 S44 MB S48 S28 S47 PDGFB	17
8	S36 BCR2L BCR S33 S1 S41 S56 LIF S37 S15 S44 MB S48 S28 S47 PDGFB	26
9	BCR2L S36 BCR S1 S33 S41 S56 LIF S37 S15 S44 S47 S28 S48 MB PDGFB	47
10	S36 BCR2L BCR S33 S1 S41 S56 LIF S37 S15 S44 S47 S28 S48 MB PDGFB	71
11	BCR2L S36 BCR S1 S33 S41 S56 LIF S37 S44 S15 S47 S28 S48 MB PDGFB	84
12	BCR2L S36 BCR S1 S33 S41 S56 LIF S37 S15 S44 MB S48 S47 S28 PDGFB	98
13	PDGFB S36 BCR2L BCR S1 S33 S41 S56 LIF S37 S15 S44 MB S48 S28 S47	107
14	S36 BCR2L BCR S1 S33 S41 S56 LIF S37 S44 S15 MB S48 S28 S47 PDGFB	124
15	S36 BCR2L BCR S33 S1 S41 S56 LIF S37 S44 S15 S47 S28 S48 MB PDGFB	126
16	BCR2L S36 BCR S1 S33 S41 S56 LIF S37 S15 S44 S28 S47 S48 MB PDGFB	144
17	S36 BCR2L BCR S33 S1 S41 S56 LIF S37 S15 S44 MB S48 S47 S28 PDGFB	147
18	S36 BCR2L BCR S1 S33 S41 S56 S37 LIF S15 S44 MB S48 S28 S47 PDGFB	159
19	S36 BCR2L BCR S1 S33 S41 S56 LIF S37 S15 S44 S48 MB S28 S47 PDGFB	175
20	BCR2L S36 BCR S1 S33 S41 S56 LIF S37 S44 S15 S28 S47 S48 MB PDGFB	211
21	S36 BCR2L BCR S33 S1 S41 S56 LIF S37 S15 S44 S28 S47 S48 MB PDGFB	216
22	S36 BCR2L BCR S1 S41 S33 S56 LIF S37 S15 S44 MB S48 S28 S47 PDGFB	238
23	S36 BCR2L BCR S1 S33 S41 S56 LIF S37 S15 S44 S47 S28 MB S48 PDGFB	311
24	S36 BCR2L BCR S33 S1 S41 S56 LIF S37 S44 S15 S28 S47 S48 MB PDGFB	317
25	BCR2L S36 BCR S33 S1 S41 S56 LIF S37 S15 S44 MB S48 S28 S47 PDGFB	421
26	S36 BCR2L BCR S1 S33 S41 S56 S37 LIF S15 S44 S47 S28 S48 MB PDGFB	436
27	S36 BCR2L BCR S1 S33 S41 S56 S37 LIF S44 S15 S47 S28 S48 MB PDGFB	516
28	S36 BCR2L BCR S1 S33 S41 S56 LIF S37 S44 S15 S47 S28 MB S48 PDGFB	553
29	S36 BCR2L BCR S41 S33 S1 S56 LIF S37 S15 S44 MB S48 S28 S47 PDGFB	618
30	S36 BCR2L BCR S41 S1 S33 S56 LIF S37 S15 S44 MB S48 S28 S47 PDGFB	649
31	S36 BCR2L BCR S1 S41 S33 S56 LIF S37 S15 S44 S47 S28 S48 MB PDGFB	653
32	S36 BCR2L BCR S1 S33 S41 S56 LIF S37 S44 S15 MB S48 S47 S28 PDGFB	710
33	S36 BCR2L BCR S1 S33 S41 S56 LIF S37 S15 S44 PDGFB MB S48 S28 S47	890
34	S36 BCR2L BCR S1 S33 S41 S56 S37 LIF S15 S44 MB S48 S47 S28 PDGFB	908
35	S36 BCR2L BCR S1 S33 S41 S56 LIF S37 S15 S44 S28 S47 MB S48 PDGFBB	912
36	S36 BCR2L BCR S1 S33 S41 S56 LIF S37 S15 S44 S48 MB S47 S28 PDGFBB	961

Note. Relative likelihood compares the maximum likelihood for the given locus order to that for the overall maximum likelihood order. Underlines indicate inversions of two or more loci relative to the best locus order; double underlines indicate more complex modifications. The DNA markers are abbreviated by deleting D22, so that D22S1 = S1.

plicated if one can use a model of equal marker retention frequency as opposed to a model of unequal marker retention frequency. In certain instances, including the present data set, the equal retention model yields estimates of distance and lod scores that are very similar to estimates obtained using the unequal retention model, even though the observed marker retention is clearly not the same for all markers (see Boehnke *et al.*, 1991). Whether this will be the case for all data sets with unequal marker retention remains to be determined.

Although the maximum likelihood approach identifies a comprehensive map of the 16 distinguishable markers that is most likely, given the data, it should be emphasized that this order of markers is not significantly more likely than a number of other map orders listed in Table 4. We are confident of the order of a set of markers only when the odds of that order are greater than 1000:1 compared to all other orders. Thus, in a practical sense, the framework map is much more useful than the comprehensive map. It is interesting to note that the most likely position of a nonframework locus with respect to flanking framework loci can differ, depending on whether one considers the nonframework locus with respect to only framework markers or with respect to both framework and nonframework markers on the comprehensive map. For example, although MB is in the D22S15–D22S28 interval on the comprehensive map, it is more likely located in the D22S28–PDFGB interval versus the D22S15–D22S28 interval with odds of 122:1 when considered solely with respect to the framework markers. Independent physical mapping information indicates that MB does indeed map between D22S28 and PDFGB (Delattre *et al.*, 1991). This example illustrates that although the comprehensive map may be the most likely map given the data, it is not always the correct map and should not be considered as such.

The region of chromosome 22 between markers D22S1 and D22S15 is known to be involved in Ewing sarcoma and neuroepithelioma, malignant small round cell tumors often associated with somatic t(11:22)(q24;q12)translocations (Budarf *et al.*, 1989). Previously, the Ewing sarcoma translocation breakpoint was mapped on chromosome 22 between flanking markers D22S1, D22S41, D22S46, D22S42, and D22S56 on the proximal side and markers LIF, D22S37, D22S44, D22S15, and D22S28 on the distal side (Budarf *et al.*, 1989; Selleri *et al.*, 1991). Because our framework RH map orders these markers, we have refined the location of the Ewing sarcoma breakpoint between the proximal marker D22S56 and the distal markers LIF and D22S37, a distance of approximately 30 cR_{8000}.

The order of the markers on the framework RH map is consistent with existing physical and genetic linkage maps of chromosome 22. Somatic cell hybrid panels of chromosome 22 have previously placed the markers used to construct our RH map into four regions (Budarf *et al.*, 1989, 1991). The markers D22S36 and BCR2L have been localized centromeric to the constitutional t(11;22) breakpoint; BCR has been mapped at the chromosome 22 breakpoint observed in chronic myelogenous leukemia (CML); D22S1, D22S33, D22S46, D22S42, and D22S41 lie between the CML and Ewing sarcoma related breakpoints; and LIF, D22S37, D22S44, D22S15, D22S28, D22S47, D22S48, MB, and PDGFB map distal to the Ewing sarcoma breakpoint. Several of the probes that lie distal to the Ewing sarcoma breakpoint have recently been linearly ordered in defined groups of markers using somatic cell hybrids: (D22S15,LIF)–(D22S28)–(MB)–(PDGFB) (Delattre *et al.*, 1991). Thus, these data assigning DNA markers to physical locations are consistent with the order of these markers in our RH framework map. Published genetic linkage maps of chromosome 22 include one by Dumanski *et al.* (1991), which consists of 40 markers; one by Rouleau *et al.* (1989), which consists of 16 markers; and one by Julier *et al.* (1988), which consists of 5 markers. These maps share in common with our RH map 4 markers (BCR, D22S1, MB, and PDGFB), 5 markers (BCR, D22S1, D22S15, D22S28 and PDGFB), and 2 markers (MB and PDGFB), respectively. Our RH framework map is consistent with the order and orientation of the markers shared with these genetic linkage maps. In some instances, the RH map provides strong support for the order of markers when other methods provide either no support or only weak support for order (i.e., the order of LIF with respect to D22S15). In other situations, another method provides strong support for an order that is only weakly supported by the RH map (i.e., the order of D22S28 with respect to MB). These comparisons of the RH map with the available physical and genetic maps of human chromosome 22 illustrate the power of using complementary methods to obtain high-resolution maps of mammalian chromosomes.

Our RH mapping data can be used to estimate the physical distance of the markers within and flanking the NF2 region. Previous comparisons of RH map distance with physical distance have not revealed any hot or cold spots of chromosome X-ray breakage distorting the relationship between RH map units and physical distance and suggest that 1 cR_{8000} corresponds to approximately 50 kb (Cox *et al.*, 1990; Burmeister *et al.*, 1991). Thus, assuming that RH mapping closely reflects physical distance, we estimate that the 302 cR_{8000} region spanned by the 16 markers that comprise the maximum likelihood comprehensive map equals a physical distance of approximately 15 Mb. Similarly, we estimate that the 126 cR_{8000} region of the map between the flanking markers of the NF2 gene, D22S1 and D22S28, represents approximately 6 Mb or 10% of the total length of the long arm of chromosome 22.

ACKNOWLEDGMENTS

We thank E. Shtivelman, D. F. Lowe, D. Mirada, R. White, P. Weller, and J. Gusella for generously providing the probes used in this study; U. Francke and M. Van Keuren, respectively, for the 380-6 and EYEF3A6 cell lines; S. Kim for technical assistance growing the radiation hybrid cell lines; and G. Duyk and H. McDermid for useful discussions and assistance in obtaining materials. R.K.W. is supported

by a National Neurofibromatosis Foundation fellowship. This research was supported by NIH Grants HG00209 and HG00376 to M.B., CA39926 and HG00425 to B.S.E., and HD24610 and HG00206 to D.R.C. and R.M.M.

REFERENCES

Barker, D., Schafer, M., and White, R. (1984). Restriction sites containing CpG show a higher frequency of polymorphism in human DNA. *Cell* **36**: 131–138.

Barker, D., Green, P., Knowlton, R., Schumm, J., Langer, E., Oliphant, A., Willard, H., *et al.* (1987). Genetic linkage map of human chromosome 7 with 63 DNA markers. *Proc. Natl. Acad. Sci. USA* **84**: 8006–8010.

Bishop, D. T., and Crockford, G. P. (1992). Comparisons of radiation hybrid mapping and linkage mapping. *Cytogenet. Cell Genet.* **59**: 93–95.

Boehnke, M., Lange, K., and Cox, D. R. (1991). Statistical methods for multipoint radiation hybrid mapping. *Am. J. Hum. Genet.* **49**: 1174–1188.

Budarf, M., Canaani, E., and Emanuel, B. S. (1988). Linear order of the four BCR-related loci in 22q11. *Genomics* **3**: 168–171.

Budarf, M., Emanuel, B. S., Mohandas, T., Goeddel, D. V., and Lowe, D. G. (1989). Human differentiation-stimulating factor (leukemia inhibitory factor, human interleukin DA) gene maps distal to the Ewing sarcoma breakpoint on 22q. *Cytogenet. Cell Genet.* **52**: 19–22.

Budarf, M. L., McDermid, H. E., Sellinger, B., and Emanuel, B. S. (1991). Isolation and regional localization of 35 anonymous DNA markers for human chromosome 22. *Genomics* **10**: 996–1002.

Burmeister, M., Suwon, K., Price, E. R., De Lange, T., Tantravahi, U., Myers, R. M., and Cox, D. R. (1991). A map of the distal region of the long arm of human chromosome 21 constructed by radiation hybrid mapping and pulsed-field gel electrophoresis. *Genomics* **9**: 19–30.

Chakravarti, A., and Reefer, J. E. (1992). A theory for radiation hybrid (Goss-Harris) mapping: Application to proximal 21q markers. *Cytogenet. Cell Genet.* **59**: 99–101.

Cox, D. R., Burmeister, M., Price, E. R., Kim, S., and Myers, R. M. (1990). Radiation hybrid mapping: A somatic cell genetic method for constructing high resolution maps of mammalian chromosomes. *Science* **250**: 245–250.

Cox, D. R., Pritchard, C. A., Uglum, E., Casher, D., Kobori, J., and Myers, R. M. (1989). Segregation of the Huntington disease region of human chromosome 4 in a somatic cell hybrid. *Genomics* **4**: 397–407.

Croce, C. M., Huebner, K., Isobe, M., Fainstain, E., Lifshitz, B., Shtivelman, E., and Canaani, E. (1987). Mapping of four distinct BCR-related loci to chromosome region 22q11: Order of BCR loci relative to chronic myelogenous leukemia and acute lymphoblastic leukemia breakpoints. *Proc. Natl. Acad. Sci. USA* **84**: 7174–7178.

Delattre, O., Azambuja, C. J., Auriss, A., Zucman, J., Peter, M., Zhang, F., Hors-Cayla, M. C., Rouleau, G., and Thomas, G. (1991). Mapping of human chromosome 22 with a panel of somatic cell hybrids. *Genomics* **9**: 721–727.

Dumanski, J. P., Carlbom, E., Collins, V. P., Nordenskjold, M., Emanuel, B. S., Wolff, R., O'Connell, P., White, R., Lalouel, J.-M., and Leppert, M. (1991). A map of 22 loci on human chromosome 22. *Genomics* **11**: 709–719.

Falk, C. T. (1991). A simple method for ordering loci using data from radiation hybrids. *Genomics* **9**: 120–123.

Feinberg, A. P., and Vogelstein, B. (1984). A technique for labeling restriction endonuclease fragments to high specific activity: Addendum. *Anal. Biochem.* **137**: 266–267.

Green, P. (1992). Construction and comparison of chromosome 21 radiation hybrid and linkage maps using CRI-MAP. *Cytogenet. Cell Genet.* **59**: 122–124.

Julier, C., Lathrop, G. M., Reghis, A., Szajnert, M. F., Lalouel, J. M., and Kaplan, J. C. (1988). A linkage and physical map of chromosome 22, and some applications to gene mapping. *Am. J. Hum. Genet.* **42**: 297–308.

Lawrence, S., Morton, N. E., and Cox, D. R. (1991). Radiation hybrid mapping. *Proc. Natl. Acad. Sci. USA* **88**: 7477–7480.

Ledbetter, S. A., Garcia-Heras, J., and Ledbetter, D. H. (1990). PCR-karyotype of human chromosomes in somatic cell hybrids. *Genomics* **8**: 614–622.

Lowe, D. F., Nunes, W., Bombara, M., McCabe, S., Ranges, G. E., Henzel, W., Tomida, M., Yamaguchi, Y. Y., Hozumi, M., and Goeddel, D. V. (1989). Genomic cloning and heterologous expression of human differentiation-stimulation factor. *DNA* **8**: 351–359.

Martuza, R. L., and Eldridge, R. E. (1988). Neurofibromatosis 2 (bilateral acoustic neurofibromatosis). *N. Engl. J. Med.* **318**: 684–688.

Richard, C. W., III, Withers, D. A., Meeker, T. C., Maurer, S., Evans, G. A., Myers, R. M., and Cox, D. R. (1991). A radiation hybrid map of the proximal long arm of human chromosome 11 containing the multiple endocrine neoplasia type 1 (MEN-1) and bcl-1 disease loci. *Am. J. Hum. Genet.* **49**: 1189–1196.

Rouleau, G. A., Kurnit, D. M., Neve, R. L., Bazanowsky, A., Patterson, D., and Gusella, J. F. (1988). D22S15—a fetal brain cDNA with BanII and SacI RFLP. *Nucleic Acids Res.* **16**: 1648.

Rouleau, G. A., Haines, J. L., Bazanowski, A., Colella, C. A., Trofatter, J. A., Wexler, N. S., Conneally, P. M., and Gusella, J. F. (1989). A genetic linkage map of the long arm of human chromosome 22. *Genomics* **4**: 1–6.

Rouleau, G. A., Seizinger, B. R., Wertelecki, W., Haines, J. L., Superneau, D. W., Martuza, R. L., and Gusella, J. F. (1990). Flanking markers bracket the neurofibromatosis type 2 (NF2) gene on chromosome 22. *Am. J. Hum. Genet.* **46**: 323–328.

Seizinger, B. R., Martuza, R. L., and Gusella, J. F. (1986). Loss of genes on chromosome 22 in tumorigenesis of human acoustic neuroma. *Nature* **322**: 644–647.

Seizinger, B. R., de la Monte, S., Atkins, L., Gusella, J. F., and Martuza, R. L. (1987). Molecular genetic approach to human meningioma: Loss of genes on chromosome 22. *Proc. Natl. Acad. Sci. USA* **84**: 5419–5423.

Selleri, L., Hermanson, G. G., Eubanks, J. H., Lewis, K. A., and Evans, G. A. (1991). Molecular localization of the t(11;22)(q24;q12) translocation of Ewing sarcoma by chromosomal in situ suppression hybridization. *Proc. Natl. Acad. Sci. USA* **88**: 887–891.

Van Keuren, M., Hart, I. M., Kao, F. T., Neve, R. L., Bruns, G. A., Kurnit, D. M., and Patterson, D. (1987). A somatic cell hybrid with a single human chromosome 22 corrects the defect in the CHO mutant ($Ade^{-}I$) lacking adenylosuccinase activity. *Cytogenet. Cell Genet.* **44**: 142–147.

Weller, P., Jeffreys, A. J., Wilson, V., and Blanchetot, A. (1984). Organisation of the human myoglobin gene. *EMBO J.* **3**: 439–446.

Zankl, H., and Zang, K. D. (1972). Cytological and cytogenetical studies on brain tumors. *Humangenetik* **14**: 167–169.

Chapter 3

Characterization of a Chromosome 22 Translocation in a Sporadic Acoustic Neuroma: Implications for Tumorigenesis

Manuscript submitted to American Journal of Human Genetics

Characterization of a Chromosome 22 Translocation in a Sporadic Acoustic Neuroma: Implications for Tumorigenesis

Kelly A. Frazer[1], Roger K. Wolff[2], Richard M. Myers[3,4] and David R.Cox[5,*]

Departments of Anatomy[1],Psychiatry[2], Physiology[3], Biochemistry and Biophysics[4], University of California, San Francisco, California, 94143; and Genetics[5], Stanford University Medical Center, Stanford, California 94305

* To whom correspondence should be addressed at Department of Genetics, Stanford University School of Medicine, Room M312, Stanford, California 94305-5120

FAX: 415-725-1534 PHONE: 415-725-8042

Running Title: Genetic analysis of an acoustic neuroma

Key Words: acoustic neuromas, chromosome 22, Neurofibromatosis Type 2

Abstract

As part of an ongoing effort to identify genes involved in the development of acoustic neuromas we used a combination of molecular and somatic cell genetic techniques to analyze chromosome 22 rearrangements in a sporadic tumor. Our data indicate that the tumor which we have characterized is monosomic for chromosome 22 and contains a reciprocal translocation in the remaining chromosome 22 homolog. Radiation hybrid mapping localizes the translocation breakpoint to a 250 kb region of chromosome 22 between DNA markers D22S347 and D22S349. This region is approximately 2 Mb distal to the Merlin gene, a recently described candidate for the NF2 tumor suppressor locus. Our results suggest that more than one chromosome 22 locus is involved in the development of acoustic neuromas.

Introduction

Acoustic neuromas are common benign tumors of the central nervous system that result from proliferation of Schwann cells along the vestibular branch of the eighth cranial nerve. The clinical symptoms frequently associated with these tumors are hearing loss, disequilibrium, and vertigo. Approximately 2000 to 3000 acoustic neuromas are diagnosed in the United States each year (Jackler and Pitts 1990). The majority of these are unilateral, nonhereditary tumors that occur sporadically in the general population. It is estimated that 5 percent of acoustic neuromas occur in individuals who have the hereditary syndrome known as Neurofibromatosis Type 2 (NF2).

NF2 is a rare autosomal dominant disorder characterized by the development of bilateral acoustic neuromas, meningiomas and other central nervous system tumors (Martuza and Eldridge 1988). Genetic linkage studies performed using NF2 pedigrees have localized the NF2 gene to a 13 cM region on the long arm of chromosome 22 between the DNA markers D22S1 and D22S28 (Rouleau et al. 1990, Narod et al. 1992). Comparisons between tumor DNA and blood DNA from NF2 patients using polymorphic chromosome 22 DNA markers have indicated that chromosome 22 rearrangements often occur in hereditary acoustic neuromas (Seizinger et al. 1987b, Fontaine et al. 1991, Wolff et al. 1992). Similar analyses of sporadic acoustic neuromas have demonstrated the same types of chromosome 22 rearrangements found in tumors from NF2 patients (Seizinger et al. 1986, Fontaine et al. 1991, Wolff et al. 1992). These data suggest that the NF2 locus is a recessive tumor suppressor gene involved in the development of both hereditary and sporadic acoustic neuromas (Seizinger et al. 1986, 1987a, 1987b).

Recently, based on studies of constitutional chromosome 22 rearrangements in NF2 patients a candidate gene for the NF2 tumor suppressor locus was identified in the proximal part of the NF2 region, near the heavy neurofilament subunit locus, NEFH (Trofatter et al. 1993). This candidate gene, Merlin, has been shown to be mutated in the germline of a number of different NF2 patients. However, to date there have not been any reports of sporadic acoustic neuromas being studied for Merlin mutations. Studies of sporadic acoustic neuromas and meningiomas have revealed chromosome 22 rearrangements both proximal and distal to the Merlin gene. A sporadic meningioma has been described that has a chromosome 22 involved in a reciprocal translocation approximately 1 Mb proximal to the Merlin gene (Lekanne Deprez et al. 1991, E.C. Zwarthoff, personal communication). Other workers have observed chromosome 22 rearrangements in acoustic neuromas and meningiomas approximately 2 Mb distal to the Merlin gene (Zhang et al. 1990a, Ahmed et al. 1991). These results suggest that there may be more than one chromosome 22 gene in the region between D22S1 and D22S28 involved in the development of these tumors.

Based on evidence for multiple sites of rearrangement between the markers D22S1 and D22S28 on chromosome 22, we are analyzing acoustic neuromas for chromosomal rearrangements in this region, in an effort to define genes involved in the development of acoustic neuromas. A high resolution map is an essential tool for detecting and localizing the position of such chromosome 22 rearrangements. In a previous report we generated a 500 kb resolution radiation hybrid map of the D22S1 to D22S28 region of chromosome 22 (Frazer et al. 1992) and we are currently using this map to search for chromosomal rearrangements in acoustic neuromas.

Most prior studies involving the analysis of acoustic neuromas for chromosome 22 rearrangements have used polymorphic markers to compare tumor DNA with blood DNA from single patients to identify the loss of chromosome 22 alleles (Seizinger et al. 1986, 1987b, Fontaine et al. 1991, Bijlsma et al. 1992, Wolff et al. 1992). This type of analysis has been limited by the degree of polymorphism of the chromosome 22 markers available for study as well as by the fact that this approach only detects those chromosomal rearrangements that result in deletions and monosomy. While other types of chromosomal rearrangements such as translocations and inversions could be detected by cytological analysis of the tumors, acoustic neuromas grow poorly in culture and are contaminated with non-tumor cells and thus are difficult to accurately karyotype (Rey et al. 1987, Couturier et al. 1990). In addition to these limitations analysis of acoustic neuromas for chromosome 22 rearrangements are often limited by the small amount of material available from each tumor.

In order to solve these problems, we have used an approach for tumor analysis which involves the fusion of tumor cells with an established hamster cell line to generate hamster-tumor hybrid cell lines. A similar approach has been used previously to analyze chromosome 22 rearrangements in a meningioma (Lekanne Deprez et al. 1991). The resulting hamster-tumor hybrids immortalize the chromosome 22 material from the tumors which allows one to karyotype the chromosomes as well as provides an unlimited source of material for molecular analysis. In addition, since these hamster-tumor hybrids segregate the two chromosome 22 homologs derived from the tumor, DNA isolated from the hybrids can be used in conjunction with both non-polymorphic and polymorphic probes to detect chromosome 22 rearrangements. In this

study, we have used a combination of hamster-tumor hybrid analysis and conventional loss of heterozygosity studies to identify abnormalities involving both copies of chromosome 22 in a sporadic acoustic neuroma. We determined that this tumor is deleted for one copy of chromosome 22 and contains a reciprocal translocation approximately 2 Mb distal to the Merlin gene in the remaining copy of chromosome 22. Our data indicate that a chromosome 22 gene distal to Merlin may be disrupted by the translocation and thus may play a role in the development of acoustic neuromas.

Materials and Methods

DNA Extraction from Tumors and Lymphoblastoid cell lines, Southern Blotting and Hybridization

High-molecular-weight DNA was isolated from the tumor tissue, lymphoblastoid cell lines, and hamster-tumor hybrids, digested to completion with restrictions enzymes, fractionated by electrophoresis, transferred to nylon membranes (Hybond N+; Amersham), hybridized with radioactive probes,washed, exposed to Kodak XAR film, and stripped of probe prior to rehybridization, as previously described (Wolff et al. 1992). Probes were radioactively labeled with [a-^{32}P]dCTP by the random primer procedure (Feinberg and Vogelstein 1984).

Production of Hamster-Tumor Hybrid Cell Lines From Tumor Cells

The tumor specimen was rinsed in Calcium Magnesium Free PBS (0.2 g/L KH_2PO_4, 2.16 g/L $Na_2HPO_47H_2O$, 0.2g/L KCL, 8.0 g/L NaCL), minced into small pieces with a razor blade, and incubated at 37°C for 25 minutes in 5 ml L15 medium containing 0.03% collagenase (Sigma, C9407), and 0.25% trypsin (Sigma, T0511). The cells were pelleted, the supernatant decanted and the procedure was repeated. After the second digestion period the cells were resuspended in 10 ml Dulbecco's Modified Eagles Medium (DMEM) containing 10% fetal calf serum (FCS), penicillin and streptomycin, and further dissociated by several cycles of trituration through a 20G hypodermic needle. Cells were preplated two times for 5 minutes each in a tissue culture Petri dish, 10 cm in diameter. Cells were plated on a tissue culture Petri dish, 10 cm in diameter and maintained in culture for 6 days. After this period, we added immortalized

A3 hamster cells to the tumor cells in order to generate hamster-tumor hybrid cell lines. Thymidine kinase (TK) deficient hamster cells were were co-cultured with the tumor cells for 12 hours at a ratio of approximately 5:1 hamster to tumor cells. We rinsed the co-cultured hamster and tumor cells twice with 10 ml serum-free DMEM media and then fused them by incubating at room temperature for 1 minute in 2 ml 50% polyethylene glycol (PEG) (Boehringer Mannheim, Cat. No. 783 641). The PEG was diluted by the addition of 10 ml serum free DMEM media and then aspirated off the plates. The cells were rinsed twice and then incubated in 10 ml serum free DMEM media at 37°C for 30 minutes. After this incubation period, the cells were trypsinized off the plates added to 10 ml HAT media (DMEM plus 100 uM hypoxanthine, 1 uM aminopterin, and 12 uM thymidine) and plated at 3.5×10^4 cells per ml to eliminate nonhybrid hamster cells and to select for hamster-tumor hybrids. Two weeks after fusion,74 independent colonies were observed, indicating a hybrid formation efficiency rate of one hybrid per 2×10^5 fused cells. Thirty-two of these hybrids were expanded and genomic DNA was isolated as previously described (Cox et al. 1990). No colonies were observed from 10^7 unfused A3 cells grown in HAT media.

In Situ Hybridization and Cytogenetics

Metaphase cells were harvested by mitotic shake-off from cultures, exposed to hypotonic solution, fixed, and dropped onto slides according to standard procedures (Trask and Pinkel 1990). To harvest a greater number of metaphase spreads, we incubated cultures in log-phase growth at 37°C for 17 hours in 10 ml DMEM media containing 10^{-7}M methotrexate, then for 5 hours in 10 ml HAT media, and then for 1 hour after addition of 0.1 ug/ml colcemid to the

HAT media. After the cells were dropped onto the slides, they were either aged for at least two weeks at room temperature or incubated for 2 hours at 65°C prior to hybridization.

The chromosomes were denatured by immersing the slides in 70% formamide, 2X SSC at pH 7.0 at 75°C for 5 minutes, dehydrated in ethanol (70%, 95%, and 100% ethanol each for 3 minutes), and then air dried. The probes were labeled by nick translation with biotin or digoxigenin (Trask and Pinkel 1990). Approximately 100 ng of probe DNA and 2.5 ug sonicated human placenta DNA in 10 ul hybridization buffer (10% dextran sulphate, 2XSSC, 50% formamide, 1% Tween 20, at pH 7.0) were denatured at 95°C for 5 minutes, incubated at 37°C for 5 hours, adjusted to a final volume of 30 ul with hybridization buffer and then applied to a denatured slide. Slides were incubated in a moist chamber at 37°C for at least 16 hours.

Following hybridization the slides were washed three times in 50% formamide, 2X SSC pH 7.0 at 42°C for 5 minutes each, and then washed three times in 2X SSC at 42°C for 5 minutes each. The slides were rinsed at room temperature in 2X SSC and then incubated for 5 minutes under a coverslip in blocking solution (0.1 M phosphate buffer, pH 8.0, 0.5%NP-40, 5%(w/v) non-fat dry milk and 0.01% Na azide) (PNM). First the biotin labeled probes were detected by incubation with Texas Red conjugated avidin (2.5 ug/ml in PNM buffer,1 hr at RT). The slides were washed in 0.005% Chaps, 2X SSC for 5 minutes at room temperature and then rinsed in 0.1 M phosphate buffer, pH 8.0, 0.5%NP-40 (PN). The digoxigenin labeled probes were then detected and the Texas Red probe signal amplified by incubation with FITC conjugated sheep anti-digoxigenin Fab fragments (15 ug/ml in PNM buffer,1 hour at room temperature), and biotin conjugated goat anti-avidin (5 ug/ml in PNM buffer,1

hour at room temperature), respectively. The slides were washed in 0.005% Chaps, 2X SSC for 5 minutes at room temperature and rinsed in PN buffer.

To amplify the FITC and Texas Red probe signals, the slides were incubated with FITC conjugated Donkey anti-Sheep IgG (20 ug/ml in PNM buffer,1 hour at room temperature) and Texas Red conjugated avidin (2.5 ug/ml in PNM buffer,1 hour at room temperature) and then washed in 0.005% Chaps, 2X SSC for 5 minutes at room temperature. The chromosomes were counterstained in 4',6-diamidino-2-phenylindole (DAPI) (0.5 ug/ml in water), rinsed in PN buffer, and then mounted in antifade solution (0.1% p-phenylenediamine dihydrochloride in glycerol, pH 8-9).

G-(trypsin-Geimsa) banding was performed according to standard procedures (Cox et al. 1982). The slides were examined with a Zeiss Neofluor (100X/1.4 N.A.) oil immersion objective lens. A 530-585 nm band pass exciter filter, a 600 nm dichroic mirror, and a 615 nm low pass filter were used. Photographs were taken using Ektachrome 400ASA color slide film.

Analysis of Radiation Hybrid Mapping Data

DNA isolated from 94 radiation hybrids previously characterized (Frazer et al. 1992) were analyzed for the retention of ten chromosome 22 loci by PCR analysis . The DNA was amplified as described below, electrophoresed through 2% agarose gels, and stained with ethidium bromide. The radiation hybrids were scored for the presence or absence of chromosome 22 loci based on the ethidium bromide staining pattern. Each radiation hybrid DNA sample was amplified by PCR in duplicate. In cases where a hybrid had inconsistent results between the duplicate runs of a particular chromosome 22 locus, the

score for that locus in that hybrid was not included in the statistical analysis. This resulted in approximately 4% incomplete data.

We constructed a Radiation Hybrid (RH) map using an equal retention model and a multipoint maximum likelihood method as previously described (Frazer et al. 1992). This method assumes that X-ray breakage occurs at random positions along the chromosome, and that fragments are retained independently. In the N-locus case, the likelihood of the RH data is a function of N-1 breakage probabilities between adjacent loci, and one or more retention probabilities. For a given locus order, breakage and retention probabilities are estimated by those values that maximize the likelihood for the RH mapping data. Orders can be compared by their maximum likelihoods, the order with the largest maximum likelihood being best supported by the data.

To identify the best locus order, we used a stepwise locus ordering algorithm that builds locus orders by adding one locus at a time while keeping under consideration at each step those partial locus orders no more than K times less likely than the current best partial locus order. We used the stepwise locus ordering algorithm with $K = 10^8$ to generate a list of 72 locus orders that have maximum likelihoods no less than one thousandth that of the comprehensive map. The comprehensive map is defined as the order of loci on this list with the highest maximum likelihood. We designated four DNA makers previously ordered relative to one another at odds of 1000 to 1 as framework markers; D22S1, LIF, D22S15, and MB (Frazer et al. 1992). Our knowledge of the order of these four framework markers allowed us to exclude 46 of the 72 locus orders on the list generated by the stepwise locus ordering algorithm.

DNA Probes used for Southern Analysis

The following chromosome 22 genes and anonymous markers were used for Southern analysis in this study: D22S1 (pMS3-18) (Barker et al. 1984), D22S9 (p22/34) (McDermid et al. 1986), D22S28 (W23C) (Rouleau et al. 1989), D22S32 (pEFZ31) (Krapcho et al. 1988), D22S33 (pH4) (Budarf et al. 1991), D22S44 (pH35) (Budarf et al. 1991), D22S46 (pH43) (Budarf et al. 1991), (D22S54) (pH85) (Budarf et al. 1991), D22S56 (pH97b) (Budarf et al. 1991), D22S164 (pMS619) (Armour et al. 1990),and D22S219 (cRWC10) (Dumanski et al. 1991).

DNA Probes Used for PCR Analysis

We selected primers for PCR amplification from published sequence for the Immunoglobulin lamda polypeptide, variable region (IGLV), Heavy neurofilament subunit (NEFH), and Leukemia inhibitory factor (LIF) genes (Table 1). We used published oligonucleotide primer sequences for the Myoglobin (MB) and cytochrome P_{450} (CYP2D) genes and the DNA marker D22S268 (Cos 75C8) (Table 1). We sequenced the DNA probes and developed oligonucleotide primers for the following anonymous chromosome 22 loci: D22S1 (pMS3-18), D22S15 (DP22), D22S346 (GT193), D22S347 (RW3-8), D22S348 (RW3-16), D22S349 (RW3-20), and D22SS350 (RW3-26) (Table 1).

The RH map was generated using the following PCR amplification conditions for all DNA markers except D22S346: 20 ng of human genomic DNA was mixed with 1.6 μmoles of each deoxyribonucleoside triphosphate, 10 ρmoles of each oligonucleotide primer, 0.25 units of *Thermus aquaticus* DNA polymerase, in 10 ul PCR buffer (2.5 mM $MgCl_2$, 50mM KCl, 20mM Tris-Cl, pH 8.3). PCR samples

were incubated at 94°C (15 seconds), 62°C (23 seconds) 72°C (30 seconds) for markers LIF, D22S1, D22S15, D22S268, D22S347, D22S348, and D22S349, and for markers MB and D22S350 at 94°C (15 seconds), 64°C (23 seconds), 72°C (30 seconds) , in a 9600 Cetus-Perkin Elmer thermal cycler for a total of 35 cycles.

PCR amplifications used for mapping the marker D22S346, and characterizing the tumor DNA and the hamster-tumor somatic cell hybrids were performed as follows: 200 ng of genomic DNA was mixed with 10 μmoles each deoxyribonucleoside triphosphate, 25 pmoles of each oligonucleotide primer, 2.5 units of *Thermus aquaticus* DNA polymerase, in 50 ul PCR buffer (1.5 mM $MgCl_2$, 50 mM KCl, 20 mg/ml gelatin, 10 mM Tris-HCl, pH 8.4). The samples were overlaid with mineral oil and incubated at 94°C, either 58°C, 60°C, 62°C, or 64°C and 72°C for 1 minute at each temperature in an automated Cetus-Perkin Elmer thermal cycler for a total of 35 cycles.

Results

Analysis of Tumor DNA

As part of our ongoing effort to define the location of genes involved in the development of acoustic neuromas we examined a sporadic acoustic neuroma for chromosomal rearrangements. The tumor had been surgically removed from a 68 years old patient with no family history of NF 2. We analyzed the acoustic neuroma for chromosome 22 deletions or complete loss of one chromosome 22 homolog (i.e. monosomy), by comparing the tumor DNA with the patient's blood DNA with 8 polymorphic chromosome 22 DNA markers, D22S1, D22S9, D22S29, D22S32, D22S33, D22S164, D22S219, and D22S346. Three of these markers, D22S9, D22S164 and D22S346, were heterozygous in the patient and thus we were able to distinguish between the alleles on the two chromosome 22 homologs in the blood DNA. In the tumor DNA, all 3 markers had lost one of the alleles present in the blood DNA, indicating that a deletion of chromosome 22 material had occurred. Because D22S9 maps proximal to the NF 2 region defined by D22S1 - D22S28 on chromosome 22 and, D22S164 and D22S346, map distal this region on chromosome 22 (Rouleau et al. 1989, Zhang et al. 1990b, Dumanski et al. 1991, K.A. Frazer, unpublished data), these data suggest that the tumor is missing a large part of one chromosome 22 homolog and that it is probably monosomic (Figure 1A). Based on these results, we suspected that the chromosome 22 homolog remaining in the tumor was structurally normal, but that it contained an undetected mutation in a tumor suppressor gene involved in the development of acoustic neuromas. However, as shown below, analysis of this chromosome 22 homolog in a hamster-tumor hybrid cell line indicated that it was structurally rearranged.

Analysis of Hybrid cell lines

In order to obtain sufficient material for an extensive analysis of the chromosome 22 homolog remaining in the tumor we captured and immortalized this chromosome in a hamster-tumor somatic hybrid cell line. We cultured tumor cells, fused them with an established hamster cell line, and isolated 31 independent hybrid cell lines (see Materials and Methods). Since the hybrid cell lines were not grown under selection requiring the retention of the chromosome 22 homolog from the tumor cells, we expected only a fraction of them to contain a human chromosome 22. To determine which hybrid cell lines had retained a human chromosome 22, we screened DNA isolated from the hybrid cell lines using PCR with DNA marker IGLV, which is located on chromosome 22 proximal to the NF 2 region (Rouleau et al. 1989, Zhang et al. 1990b, Delattre et al. 1991, Dumanski et al. 1991). Thirteen of the thirty-one independent hybrid cell lines scored positive for the IGLV marker, indicating that they contained a human chromosome 22.

Acoustic neuromas are frequently contaminated with fibroblasts which contain both human chromosome 22 homologs. Therefore to assess the success of our approach in specifically capturing the chromosome 22 homolog derived from the tumor we analyzed the thirteen hybrid cell lines with the polymorphic D22S346 marker. These data showed that four of the hybrids contained both D22S346 alleles, and that four contained only the allele not present in the tumor. Therefore these eight hybrids must have resulted from fusion of the hamster cells with contaminating fibroblasts and not with the tumor cells. In contrast, the other five hybrid cell lines were possibly derived from the tumor. Three of these hybrid cell lines contained the D22S346 allele present in the tumor while two, cell lines A6-1 and A5-3, which had scored positive for the IGLV marker, did not contain any

D22S346 allele (Figure 1A). We had anticipated capturing only structurally normal chromosome 22 homologs because our analysis of the tumor DNA suggested it was monosomic for chromosome 22. Therefore these hybrid cell lines which contained the IGLV marker but were deleted for the D22S346 marker were an unexpected finding and suggested the chromosome 22 homolog remaining in the tumor was structurally rearranged (Figure 1B).

Our data were consistent with the tumor containing either a balanced translocation in a single chromosome 22 homolog or structural rearrangements involving both chromosome 22 homologs. To determine if the chromosomal rearrangements in the tumor involved one or both chromosome 22 homologs, we analyzed D22S9 and D22S346 alleles in the tumor DNA. If the hemizygosed alleles in the tumor DNA are on the same chromosome 22 in normal cells (i.e. in phase), this would suggest the chromosomal rearrangement involved a single chromosome 22 and was a balanced translocation. By contrast, if the two hemizygosed alleles are on different chromosome 22 homologs in normal cells (i.e. not in phase), this would indicate that in the tumor DNA both chromosome 22 homologs were rearranged. Since our data revealed that several of the hybrid cell lines were generated by fusion with normal human cells, we were able to analyze the segregated chromosome 22 homologs in these cell lines to determine the phase of the D22S9 and D22S346 alleles in the patient. As shown in Figure 1, the alleles of D22S9 and D22S346 retained in the tumor DNA are present in cell line B8-2 which contains a single copy of chromosome 22 derived from a normal cell. In addition, cell line A6-1, which contained no D22S346 allele, retained the same allele of D22S9 present in the tumor DNA, supporting our hypothesis that the rearranged chromosome was derived from the tumor. Together these data suggest that the chromosomal rearrangement present in cell

lines A6-1 and A5-3 most likely is a balanced translocation involving a single chromosome 22 homolog.

Characterization of Chromosome 22 rearrangement

To define more precisely the location of the chromosome 22 rearrangement detected in hybrid A6-1, we screened DNA isolated from this hybrid cell line with 17 DNA markers and genes on chromosome 22 that had previously been ordered relative to one another. Radiation hybrid mapping (RH mapping), genetic linkage analysis, and physical mapping techniques had placed markers IGLV, D22S9,and D22S219 proximal to the NF2 region, ordered the following markers in the NF2 region, (D22S1,D22S33, D22S46) - D22S56 - (NFH, D22S268 , LIF) - (D22S15, D22S44) - (MYO, D22S28), and placed markers CYP2D, and D22S54 distal to the NF2 region (Rouleau et al. 1989, Delattre et al. 1991, Dumanski et al. 1991, Frazer et al. 1992, Marineau et al. 1992b, K.A. Frazer, unpublished data). DNA markers D22S347, D22S349, D22S350, D22S348 and D22S346 were known to lie in the NF2 region but had not previously been ordered (R.K. Wolff, unpublished data). The tumor hybrid cell line A6-1 scored positive for twelve probes, IGLV, D22S9, D22S219, D22S1, D22S33, D22S46, D22S56, NEFH, D22S268, LIF, D22S15, and D22S347, while eight probes were absent, D22S44, D22S350, D22S348, MB, D22S28, D22S346, CYP2D, and D22S54 (data not shown). These data showed that all DNA markers previously mapped proximal to D22S15 were retained and all markers which mapped distal to D22S44 were absent, indicating that the chromosome 22 rearrangement occurred within the NF2 region, between DNA markers D22S15 and D22S44.

In an effort to refine the location of the chromosome 22 rearrangement, we constructed an RH map to determine if any of the markers placed but not previously ordered in the NF2 region were the closest flanking markers. We used PCR to screen DNA isolated from 94 independent radiation hybrids containing fragments of human chromosome 22 for the presence or absence of ten human chromosome 22 specific loci, resulting in the RH map in Figure 2A. Since the hybrid cell line A6-1 had retained marker D22S347 but was missing marker D22S349, the chromosome 22 rearrangement in the NF2 region can be placed between between DNA markers D22S347 and D22S349, a distance of approximately 250 kb (Figure 2B).

Chromosome 22 rearrangement in the NF2 region identified as a translocation

To test our hypothesis that the rearranged chromosome 22 captured in cell line A6-1 consisted of a balanced translocation in the NF2 region, we performed *in situ* hybridization and G-banding analysis. We simutaneously hybridized metaphase spreads of the A6-1 cell line with digoxigenin-labeled D22S347 cosmid and biotin-labeled D22S349 cosmid and then detected and amplified the probes as described in Material and Methods. After analyzing numerous metaphase spreads of this cell line, we determined that the D22S347 cosmid hybridized to the center of a small acrocentric-shaped chromosome and, as expected, that the D22S349 cosmid did not specifically hybridize to any chromosome (Figures 3F, 3G, and 3H). This finding supports the hypothesis that the chromosomal rearrangement is a translocation. If it were a terminal deletion, the D22S347 probe, shown by RH mapping to lie within 250 kb of the rearrangement, would have hybridized at the distal end of the derivative chromosome 22.

Based on our translocation hypothesis the hybrid cell lines, B8-2, C6-1, and C4-1,which had retained the D22S349 marker and only the allele of D22S346 present in the tumor, were either derived from the tumor and contained both halves of the chromosome 22 translocation or were derived from fibroblasts and contained a normal human chromosome 22. To ascertain if we had captured the distal half of the chromosome 22 translocation in one of these hybrid cell lines we performed *in situ* hybridization using the D22S347 and D22S349 cosmids as probes. In all three cell lines the D22S347 cosmid and the D22S349 cosmid had identical patterns of hybridization indicating that a normal chromosome 22 had been captured (fig. 3C, 3D, and 3E) .

To compare the relative size of the derivative chromosome 22 with a normal human chromosome 22, we hybridized metaphase spreads of the A6-1, A5-3, B8-2, C6-1, and C4-1 cell lines, with biotin-labeled total human probe followed by detection with avidin-conjugated to FITC. In the A6-1 and A5-3 cell lines only one small acrocentric-shaped human chromosome was observed per metaphase spread (Figures 3A and 3B). Analysis of the five cell lines hybridized with the total human probe indicated that the acrocentric-shaped derivative chromosome captured in cell lines A6-1 and A5-3 is slightly larger than a normal human chromosome 22. The total human probe hybridized to both the proximal and distal halves of the acrocentric shaped derivative chromosome 22 indicating that it is composed entirely of human material (Figures 3A and 3B). Analysis of the A6-1 and A5-3 hybrid cell lines showed that they contain different human chromosomes (data not shown). Based on these data and the fact that cell lines A6-1 and A5-3 were selected from different petri dishes, we believe that these hybrids are derived from two independent fusion events. These data provide additional support of our hypothesis that the chromosomal rearrangement is a

translocation derived from the acoustic neuroma and not an artifact of tissue culture.

To determine if the translocated chromosome 22 appeared rearranged cytologically we G-(trypsin-Geimsa) banded metaphase spreads of the A6-1 cell line. We discovered that the acrocentric-shaped derivative chromosome 22 had a dark band in the distal half of the long arm which is not the banding pattern of a normal human chromosome 22 (Figures 3I and 3J). Although a deletion distal to the q12.2 band of chromosome 22 would have resulted in this pattern, this would be inconsistent with the size, and the fact that the D22S347 cosmid is located in the center, of the derivative chromosome. Therefore, we believe that this dark band is material from an as-yet unidentified human chromosome involved in a reciprocal translocation with the derivative chromosome 22. These results are consistent with our hypothesis that the tumor DNA contained a balanced chromosome 22 translocation and that the hybrid cell line A6-1 captured the proximal half of this derivative chromosome 22.

Discussion

Our laboratory is analyzing acoustic neuromas for chromosomal rearrangements in an effort to identify genes that play a role in the development of these tumors. In this report, we describe the characterization of chromosome 22 rearrangements detected in a sporadic acoustic neuroma.

The ability to extensively analyze acoustic neuromas for chromosomal rearrangements is limited by the fact that only a small amount of DNA is isolated from each tumor. To avoid running out of tumor material, we have made it a standard component of our protocol to fuse cultured tumor cells with an established hamster cell line. This procedure immortalizes the chromosome 22 material from the tumor in the resulting hamster-tumor somatic cell hybrids. Any informative polymorphic chromosome 22 probe can be used to determine which hybrids have retained and segregated the chromosome 22 homologs from one another. The availability of separated chromosome 22 homologs then enables one to use non-polymorphic markers to detect chromosomal rearrangements by simply screening for their presence or absence in the hybrid cell lines containing only one chromosome 22 homolog. Since this procedure does not actively select for the retention of chromosome 22, one could use this approach to immortalize any human chromosome derived from tumor material. These hamster-tumor hybrids are relatively easy to generate; however a considerable amount of time is required to grow and isolate DNA from each one. Therefore, to reduce the amount of work initially involved, our standard approach is to freeze the hamster-tumor fusion plate as a single mass culture. Individual hamster-tumor hybrid clones can then be isolated at a later date as desired.

In this study, we were surprised to find both copies of chromosome 22 in hamster-tumor hybrids, since the molecular analysis of the tumor DNA indicated that the tumor was monosomic for chromosome 22. This finding suggests that some of the hybrid cell lines retained one or more copies of human chromosome 22 derived from non-tumor cells present in the tumor material. It is extremely difficult to distinguish between a chromosome 22 captured from tumor cells and from non-tumor cells in the absence of a gross structural rearrangement of the captured chromosome. The possibility that chromosomes from both tumor and non-tumor cells may be captured in the hamster-tumor hybrids needs to be taken into account when tumors are analyzed by this approach. Despite this drawback, the hamster-tumor hybrid approach should provide a useful method for analyzing chromosomal rearrangements in a variety of tumors in which the cells are difficult to grow in culture.

Our analysis of the rearranged chromosome 22 captured in hamster-tumor hybrid A6-1 is consistent with it being derived from the tumor. Because this derivative chromosome 22 was isolated in two independent hybrid cell lines, it is unlikely to be an artifact of tissue culture. In situ hybridization indicates that a significant amount of human material lies distal to the D22S347 cosmid on the derivative chromosome 22 in hybrid cell line A6-1. This finding, combined with the fact that D22S347 is within an estimated 250 kb of the chromosomal rearrangement, is inconsistent with a terminal deletion. The data are consistent with the interpretation that the derivative chromosome 22 represents a translocation with an as-yet unidentified human chromosome. The fact that the tumor DNA contains chromosome 22 markers distal to D22S347 derived from a single chromosome 22 homolog suggests that this translocation in the tumor is reciprocal, and that the tumor retains both halves of the translocation, while the

tumor hybrid retains only the derivative chromosome 22. This study shows the power of using molecular and cytogenetic approaches in parallel to study chromosomal rearrangements in tumors. Neither approach used in isolation would have determined that the acoustic neuroma had lost one copy of chromosome 22 while retaining both halves of a reciprocal translocation of the remaining chromosome 22 homolog.

We believe that the chromosome 22 translocation described in this report most likely interrupts expression of a gene involved in the development of acoustic neuromas. Preliminary sequence analysis has indicated that the primary structure of the Merlin gene remaining in the sporadic acoustic neuroma was not mutated. (R.K. Wolff , manuscript in preparation). These data support our hypothesis that a second locus is likely to be interrupted by the translocation and is responsible for the development of this tumor. The fact that acoustic neuromas rarely contain nonspecific chromosomal rearrangements (Seizinger et al. 1986, Couturier et al. 1990) argues against the possibility that the translocation we have identified is a coincidental rearrangement that played no role in the development of the tumor. Furthermore, the translocation occurs in a region of chromosome 22 in which other rearrangements have been detected in sporadic acoustic neuromas and in a meningioma (Zhang et. al, 1990a, Ahmed et al. 1991). Based on our RH map, the chromosomal rearrangements detected in these tumors are located approximately 2 Mb distal to the Merlin gene.

Hybrids A6-1 and A5-3 should provide a valuable reagents for further studies aimed at isolating the translocation breakpoint described here and defining genes whose function or expression is altered by this chromosomal rearrangement.

References

Abbott and Povey (1991) Development of human chromosome-specific PCR primers for characterization of somatic cell hybrids. Genomics 9:73-77

Ahmed FB, Maher ER, Affara NA, Bentley E, Xuereb JH, Rouleau GA, Hardy D, David M, Ferguson-Smith MA (1991) Deletion mapping in acoustic neuroma. Cytogenet Cell Genet HGM11:203

Anderson MLM, Szajnert MF, Kaplan JC, McColl L, Young BD (1984) The isolation of a human Ig V-lambda gene from a recombinant library of chromosome 22 and estimation of its copy number. Nucleic Acids Res. 12:6647-6661

Armour JAL, Povey S, Jeremiah S, Jeffreys AJ (1990) Systematic cloning of human minisatellites from ordered array charomid libraries. Genomics 8:501-512

Barker D, Schafer M, White R (1984) Restriction sites containing CpG show a higher frequency of polymorphism in human DNA. Cell 36:131-138

Bijlsma EK, Brouwer-Mladin Roma, Bosch DA, Westerveld A, Hulsebos TJM (1992) Molecular characterization of chromosome 22 deletions in schwannomas. Genes Chromosom Cancer 5:201-205

Budarf ML, McDermid HE, Sellinger B, Emanuel BS (1991) Isolation and regional localization of 35 unique anonymous DNA markers for human chromosome 22. Genomics 10:996-1002

Couturier J, Delattre O, Kujas M, Philippon J, Peter M, Rouleau G, Aurias A, Thomas G (1990) Assessment of chromosome 22 anomalies in neurinomas by combined karyotype and RFLP analyses. Cancer Genet Cytogenet 45:55-62

Cox DR, Sawicki JA, Yee D, Appella E, Epstein CJ (1982) Assignment of the gene for beta 2-microglobulin ($\beta 2\mu$) to mouse chromosome 2. PNAS 79(6):1930-4

Cox DR, Burmeister M, Price ER, Kim S, Myers RM (1990) Radiation hybrid mapping: A somatic genetic method for constructing high resolution maps of mammalian chromosomes Science 250:245-250

Delattre O, Azambuja CJ, Aurias A, Zucman J, Peter M, Zhang F, Hors-Caya MC, Rouleau G, Thomas G (1991) Mapping of human chromosome 22 with a panel of somatic cell hybrids. Genomics 9:721-727

Dumanski JP, Carlbom E, Collins VP, Nordenskjold M, Emanuel BS, Budarf ML, McDermid HE, Wolff R, O'Connell P, White R, Lalouel J-M, Lepper M (1991) A map of 22 loci on chromosome 22. Genomics 11:709-719

Feinberg AP, Volgelstein B (1984) A technique for labeling restriction endonuclease fragments to high specific activity. Anal Biochem 137:266-267

Fontaine B, Sanson M, Delattre O, Menon AG, Rouleau GA, Seizinger BR, Jewell AF, Hanson MP, Aurias A, Martuza RL, Gusella JF, Thomas G (1991) Parental origin of chromosome 22 loss in sporadic and NF2 neuromas. Gemonics 10:280-283

Frazer KA, Boehnke M, Budarf ML, Wolff RK, Emanuel BS, Myers RM, Cox DR (1992) A radiation hybrid map of the region on human chromosome 22 containing the neurofibromatosis type 2 locus. Genomics 14, 574-684

Gough AC, Miles JS, Spurr NK, Moss JE, Gaedigk A, Eichelbaum M, Wolf CR (1990) Identification of the primary gene defect at the cytochrome P_{450} *CYP2D* locus. Nature 347:773-776

Jackler RK, Pitts LH (1990) Acoustic Neuroma. Neurosurg Clin North Am 1:199-223

Krapcho K, Nakamura Y, Fujimoto E, Eldridge R, Leppert M, O'Connell P, Lathrop GM, Lalouel J-M, White R (1988) Isolation and mapping of a polymorphic DNA sequence (pEFZ31) on chromosome 22 (D22S32). Nucleic Acids Res. 16:5221

Lekanne Deprez RH, Groen NA, van Biezen NA, Hagemeijer A, van Drunen E, Koper JW, Avezaat CJJ, Bootsma D, Zwarthoff EC (1991) A t(4;22) in a meningioma points to the localization of a putative tumor-suppressor gene. Am J Hum Genet 48:783-790

Ledbetter SA, Garcia-Heras J, Ledbetter DH (1990) PCR-karyotype of human chromosomes in somatic cell hybrids. Genomics 8:614-622

Lees JF, Shneidman PS, Skuntz F, Carden MJ, Lazzarini RA (1988) The structure and organization of the human heavy neurofilament subunit (NF-H) and the gene encoding it. EMBO J 7:1947-1955

Marineau C (1992a) Genome Data Base (GDB), Welch Medical Library, 1830 East Monument Street, Baltimore, MD 21205

Marineau C, Baron C, Parboosingh J, Narod S, Sanson M, Lenoir G, Aurias A, Desmaze C, Delattre O, Thomas G, Rouleau GA (1992b) Detection of a germline deletion on chromosome 22 in a Neurofibromatosis Type 2 family. Am J Hum Genet 51(4):A64

Martuza RL, Eldridge R (1988) Neurofibromatosis 2 (bilateral acoustic neurofibromatosis). N Engl J Med 318:684-688

McDermid HE, Duncan AMV, Brasch KR, Burn J, Holden JJA, Magenis E, Sheehy R, Burn J, Kardon N, Schinzel A, Teshima I, White BN (1986) Characterization of the supernumerary chromosome in Cat Eye Syndrome. Science 232:646-648

Moreau J-F, Donaldson DD, Bennett F, Witek-Giannotti J, Clark SC, Wong GG (1988) Leukaemia inhibitory factor is identical to the myeloid growth factor human interleukin of DA cells. Nature 336:690-692

Narod SA, Parry DM, Parboosingh J, Lenoir GM, Ruttledge M, Fischer G, Eldridge R, Martuza RL, Frontali M, Haines J, Gusella JF, Rouleau GA (1992) Neurofibromatosis type 2 appears to be a genetically homogeneous disease. Am J Hum Genet 51:486-496

Rey JA, Bello MJ, de Campos JM, Kusak E, Moreno S (1987) Cytogenetic analysis in human neurinomas. Cancer Genet Cytogenet 28:187-188

Rouleau GA, Kurnit DM, Neve RL, Bazanowsky A, Patterson D, Gusella JF (1988) D22S15--a fetal brain cDNA with BanII and SacI RFLP. Nucleic Acids Res. 16:1648

Rouleau GA, Haines JL, Bazanowski A, Colella CA, Trofatter JA, Wexler NS, Conneally PM, Gusella JF (1989) A genetic linkage map of the long arm of human chromosome 22. Genomics 4:1-6

Rouleau GA, Seizinger BR, Wertelecki W, Haines JL, Superneau DW, Martuza RL, Gusella JF (1990) Flanking markers bracket the neurofibromatosis type 2 (NF2) gene on chromosome 22. Am J Hum Genet 46:323-328

Seizinger BR, Martuza RL, Gusella JF (1986) Loss of genes on chromosome 22 in tumorigenesis of human acoustic neuromas. Nature 322:644-647

Seizinger BR, de la Monte S, Atkins L, Gusella JF, Martuza RL (1987a) Molecular genetic approach to human meningioma: loss of genes of chromosome 22. Proc Natl Acad Sci USA 84:5419-5423

Seizinger BR, Rouleau GA, Ozelius LJ, Lane AH, St George-Hyslop P, Huson S, Gusella JF, Martuza RL (1987b) Common pathogenetic mechanism for three tumor types in bilateral acoustic neurofibromatosis. Science 236:317-319

Trask B, Pinkel P (1990) Fluorescence in situ hybridization with DNA probes. Methods in Cell Biology 33:383-400

Trofatter JA, MacCollin MM, Rutter JL, Murrell JR, Duyao MP, Parry DM, Eldridge T, Kley N, Menon AG, Pulasid K, Hasse VH, Ambroae DM, Munroe D, Bove C, Haines JL, Martuza RL, MacDonald ME, Seizinger BR, Short MP, Buckler AJ, Gusella JF (1993) A novel moesin-, exrin-, radixim-like gene is a candidate for the neurofibromatosis 2 tumor suppressor. Cell 72: 791-800

Van Keuren M, Hart IM, Kao FT, Neve RL, Bruns GA, Kurnit DM, Patterson D (1987) A somatic cell hybrid with a single human chromosome 22 corrects the defect in the CHO mutant (Ade-I) lacking adenylosuccinase activity. Cytogenet. Cell Genet. 44:142-147

Wolff RK, Frazer KA, Jackler RK, Lanser MJ, Pitts LH, Cox DR (1992) Analysis of chromosome 22 deletions in neurofibromatosis type2-related tumors. Am J Hum Genet 51:478-485

Wolff RK (1993) Genome Data Base (GDB), Welch Medical Library, 1830 East Monument Street, Baltimore, MD 21205

Zhang FR, Delattre O, Rouleau G, Couturier J, Lefrancoid D, Thomas G, Aurias A (1990a) The neuroepithelioma breakpoint on chromosome 22 is proximal to the meningioma locus. Genomics 6:174-177

Zhang FR, Aurias A, Delattre O, Stern MH, Benitez J, Rouleau G, Thomas G, (1990b) Mapping of human chromosome 22 by *in situ* hybridization. Genomics 7:319-324

Table 1

Primers for Amplification of DNA by PCR

Locus	Sequence (5' to 3')	Size (bp)[a]	Reference
IGLV	forward: CTGCTTCCTCCCACAGGACAAATCCACAGC	340	Anderson et al. 1984
	reverse: CAGACACATGTTAGAAATTAGAAGGGCAGA		
NEFH	forward: CTCAGAAGAGTCCCGGAGCTCAAGGATCAG	595	Lees et al. 1988
	reverse: GTCTGGGGTGTCACATCCAGACCTCCCCTG		
LIF	forward: CCGAGGGATCTCAGGAGTTGGGTGC	512	Moreau et al. 1988
	reverse: GAAGACAGCCTTCCATCCCAGAGGC		
MB	forward: ACTTGAACTCTAGTCTGGCTGCCCC	471	Abbott and Povey 1991
	reverse: CAAAGTGGGTGGCAGTCCCCTTTAC		
CYP2D	forward: CGCCTTCGCCAACCACTCCG	334	Gough et al. 1990
	reverse: AAATCCTGCTCTTCCGAGGC		

Table 1 - continued

Locus	Sequence (5' to 3')	Size (bp)	Reference
D22S268	forward: TACGTCCTCACAATCCAGCGT reverse: CTGAGGTGGGAGGATTAC	≈250	Marineau 1992a
D22S1	forward: GGTGATGAGAT(G/T)AGGTCTCATCCA reverse: CTGGATGGTGAAGAATGGAGATCA	≈600	Barker et al. 1984
D22S15	forward: TGGACCCTGTATTAACAGAAGCAACTC reverse: GGCTCTTTTTCACCAGAACAACGACC	≈580	Rouleau et al. 1988
D22S346	forward: CCAGCCTTGAGAGGTTAGAATGGC reverse: GTGGACTGTTAATTTCTAGAATTGCC	≈150	Wolff 1993
D22S347	forward: TGGTGAATGTGACATTCATGGTCT reverse: CAGAGTAAGGAGGCAAGATAGTGC	550	Wolff 1993

Table 1 - continued

Locus	Sequence (5' to 3')	Size (bp)	Reference
D22S348	forward: TCCCCGTCTGTGCTCTGTACTTGTT	199	Wolff 1993
	reverse: GTCTTTCTTCCTCATTTTGGCCTTG		
D22S349	forward: CCGTTCCCTGTTATTCCAGCTCTAC	143	Wolff 1993
	reverse: GATGAATTTCTTAGCACACTAGGCC		
D22S350	forward: CTAGTCCTGACTCCCACAGCTGGC	229	Wolff 1993
	reverse: CCAACATAATCCAGCCCCCATCATC		

[a] Expected size of amplified DNA producrt

Figure Legends

Figure 1. A, Analysis of genomic DNA isolated from blood, tumor tissue and four somatic cell hybrid cell lines, A6-1, B7-2, B8-2, and A8-1, containing one or more copies of human chromosome 22 derived from the tumor. Southern blot analysis using marker D22S9 and PCR analysis using marker D22S346 shows that in the tumor DNA both markers are missing an allele present in the blood DNA. Cell line A6-1 retained the allele of D22S9 present in the tumor but did not contain any D22S346 allele, cell line B7-2 retained both alleles of D22S9 and D22S346, cell line B8-2 retained the alleles of D22S9 and D22S346 present in the tumor DNA, and cell line A8-1 retained the alleles of D22S9 and D22S346 not present in the tumor DNA. Based on this analysis hybrid cell lines B7-2 and A8-1 resulted from fusion of hamster cells with normal human fibroblasts. Therefore these results indicate that the alleles of D22S9 and D22S346 present in the tumor DNA represent a single homolog of chromosome 22. B, Schematic diagram illustrating the status of chromosome 22 material present in blood, tumor cells, and hamster-tumor hybrid cell line A6-1. Our data indicates that both chromosome 22 homologs are structurally normal in non-tumor cells. In the tumor DNA the hemizygosed alleles of DNA markers D22S9 and D22S346 are derived from the same chromosome 22 homolog suggesting that the tumor is monosomic for chromosome 22. Hybrid cell line A6-1 contains the allele of D22S9 present in the tumor DNA but contains no D22S346 allele indicating that it has captured a structurally rearranged chromosome 22. These data are consistent with the tumor containing a balanced translocation involving a single chromosome 22 homolog and the hybrid cell line A6-1 retaining the proximal half of this derivative chromosome 22.

Figure 2. A, The order of the markers in the comprehensive Radiation hybrid map constructed using an equal retention model and a maximum likelihood method (see Materials and Methods). Distances between the markers are indicated in cR_{8000} to the left of the diagram. The markers D22S268 and LIF had no breaks between them and therefore we are unable to determine their relative order. In this system 1 cR_{8000} is equal to a frequency of 1 percent breakage between two markers after exposure to 8000 rad of X-rays. Previous analysis of these hybrids has shown that 1 cR_{8000} equals approximately 50 kb (Frazer et al. 1992). The four groups of DNA markers, as defined by the shaded boxes, are ordered relative to one another at 1000:1 odds as determined by likelihood ratios. For example, the two markers S347 and S349 are located between the marker in the proximal shaded box, S15, and the markers in the distal shaded box, MB, S350, S348, S346, at 1000:1 odds. The DNA markers are abbreviated by deleting D22, so that D22S1 equals S1. B, Analysis of hybrid cell line A6-1 with markers S347 and S349 indicating that the chromosome 22 rearrangement occurred in the NF2 region. Lane 1 contains DNA amplified from cell line EYEF3A6 (GM10027), a hamster-human hybrid cell line containing an intact human chromosome 22 and fragments of human chromosomes 15 and 19 (Van Keuren et al. 1987, Ledbetter et al. 1990). Lanes 2 and 3 contain DNA amplified from the hamster-tumor hybrid cell line A6-1 and the hamster cell line A3, respectively. This data demonstrates that hybrid cell line A6-1 retains marker S347 but is missing marker S349 and therefore localizes the chromosome 22 rearrangement in the NF2 region between these two markers.

Figure 3. Analysis of hamster-tumor hybrid cell lines containing rearranged and normal chromosomes 22 by FISH and G-banding. A complete metaphase spread of cell line A6-1 stained with Dapi (panel A) and hybridized with a total human DNA probe (panel B) which distinguishes the 10 human chromosomes present in this hybrid cell line from the hamster chromosomes. Of these 10 human chromosomes only one, indicated by the arrow, is a small acrocentric chromosome.

A partial metaphase spread of the hamster-tumor hybrid cell line B8-2 which contains a normal human chromosome 22 is stained with Dapi (panel C), hybridized with the S347 cosmid (panel D) and hybridized with the S349 cosmid (panel E). The S347 and S349 cosmids both specifically hybridize to the same location on the normal human chromosome 22, indicated by the arrows, and have identical background hybridization patterns on the other human chromosomes.

A partial metaphase spread of cell line A6-1 stained with Dapi (panel F), hybridized with the S347 cosmid probe (panel G), and hybridized with the S349 cosmid probe (panel H). Although all human chromosomes in this hybrid show faint signal with these probes, the S347 cosmid specifically hybridizes to the center of the small acrocentric human chromosome, indicated by the arrows. Note that no specific signal is observed with the S349 cosmid.

G-banding of cell line A6-1 shows that the acrocentric shaped derivative chromosome 22 has a dark band in the distal half of the long arm (panel I) which is not in the G-banded normal human chromosome 22 present in the metaphase spread of a lymphoblast cell line (panel J).

Figure 1

A.

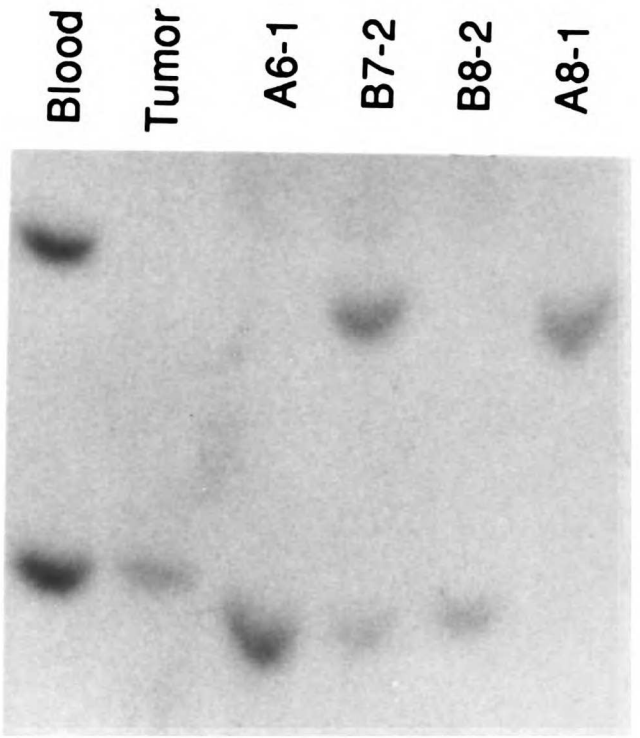

D22S9

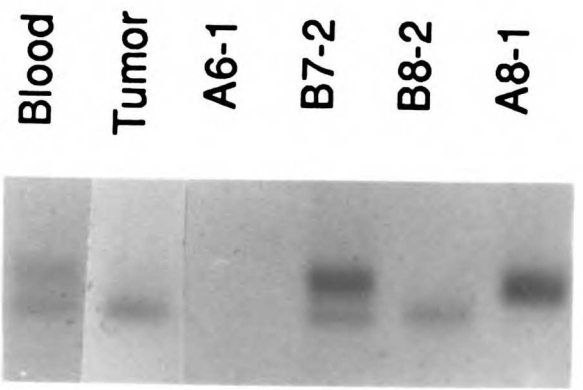

D22S346

B.
Germline
(Blood)
Chromosome 22
Chromosome ?
D22S9
D22S346
Tumor
Chromosome 22
Chromosome ?
D22S9
D22S346
Hamster-Tumor Hybrid
(A6-1)
Chromosome 22
D22S9

Figure 1

Figure 2

A.

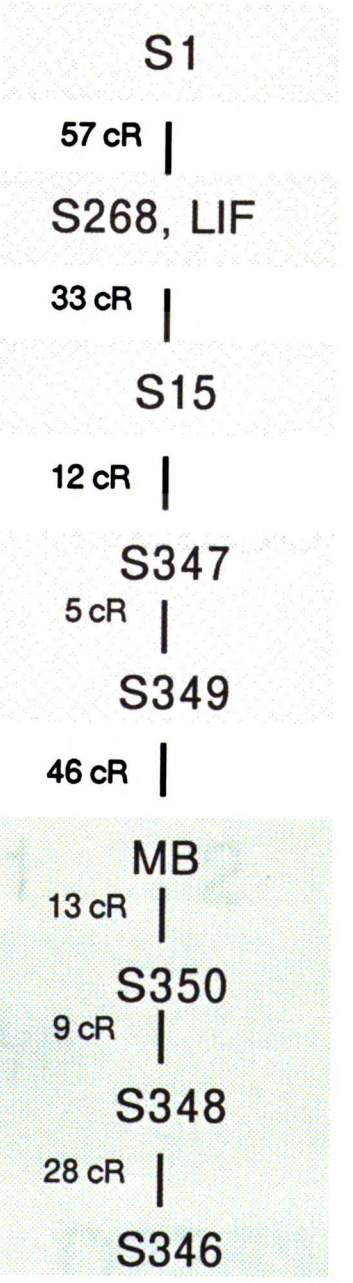
S1
57 cR
S268, LIF
33 cR
S15
12 cR
S347
5 cR
S349
46 cR
MB
13 cR
S350
9 cR
S348
28 cR
S346

Figure 2

B.

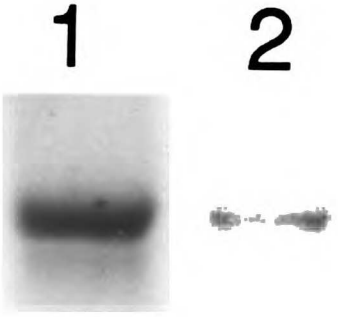

D22S347

1 2 3

D22S349

Figure 3

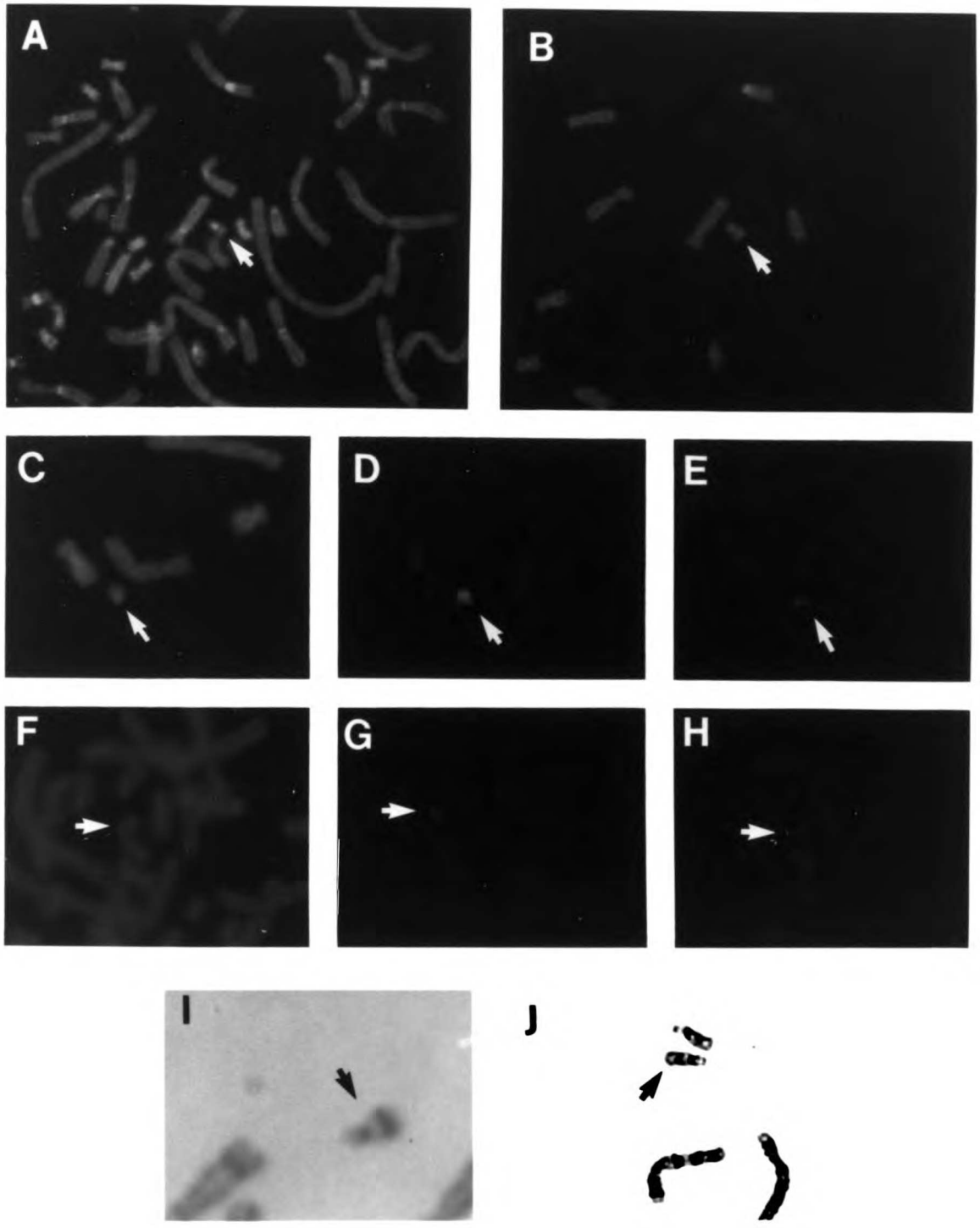

Chapter 4

Efforts to Isolate a Translocation Breakpoint.

Kelly A. Frazer

Department of Anatomy
University of California at San Francisco
San Francisco, California 94143

Abstract

Acoustic neuromas are common intracranial tumors occurring in humans. As part of an effort to clone genes involved in the development of these tumors, I previously identified a sporadic acoustic neuroma that contains a reciprocal chromosome 22 translocation. Our data suggest that this chromosome 22 translocation may alter the expression of a gene involved in the development of acoustic neuromas. In an attempt to clone this gene, I isolated DNA from the estimated 250 kb genomic region between the loci which flank the translocation, D22S347 and D22S349. Six YAC clones were isolated by screening two YAC libraries with sequence-tagged sites (STSs) generated from the loci D22S247 and D22S249. To establish the order of the YAC clones and to simultaneously convert them into more easily manipulated cosmid clones, I used the YACs as probes to screen a sub-chromosome 22 specific cosmid library. The isolated cosmids were grouped into defined regions, referred to as bins, based on their hybridization patterns with the overlapping YACs, and were further analyzed by YAC end and cosmid hybridization experiments. The cosmids isolated with the YACs at the D22S347 locus were placed into 6 separate bins, spanning a distance of approximately 350 kb. Screening the cosmid library with the YACs at the D22S349 locus combined with YAC end and cosmid hybridization experiments, resulted in an ordered array of cosmids consisting of 8 bins that also spans a distance of approximately 350 kb. These two sets of binned cosmids at the D22S347 and D22S349 loci did not overlap with each other. To establish if either set crossed the translocation breakpoint, I used cosmids located in the left and right end bins at the D22S347 and D22S349 loci as hybridization probes on Southern blots containing the derivative chromosome 22. I determined that neither set of cosmids crossed the

chromosome 22 translocation, however my data indicates that the breakpoint is most likely located within 50 kb of the cosmids in the left end bin at the D22S349 locus. The YAC and cosmid clones at the D22S347 and D22S349 loci provide reagents for the isolating the chromosome 22 gene that is affected by the translocation breakpoint and characterizing its role in the development of nervous system tumors.

Introduction

Acoustic neuromas, the commonly used term for Schwannomas of the eighth cranial nerve, account for approximately 8 percent of all intracranial tumors (Jackler and Pitts, 1990). Although the majority of acoustic neuromas arise in the general population as sporadic unilateral tumors, approximately 5 percent of acoustic neuromas occur as bilateral tumors in individuals with the hereditary syndrome known as Neurofibromatosis Type 2 (NF2) (Jackler and Pitts, 1990). In addition to bilateral acoustic neuromas, NF2 patients frequently develop other types of nervous system tumors, including meningiomas, gliomas, and spinal neurofibromas.

Analysis of hereditary and sporadic acoustic neuromas has demonstrated specific loss of heterozygosity for polymorphic chromosome 22 DNA markers, indicating the involvement of chromosome 22 in the development of these tumors. Based on chromosome 22 constitutional deletions in NF2 patients, a candidate gene for the NF2 locus, Merlin, has recently been cloned (Trofatter et al., 1993) Hereditary and sporadic acoustic neuromas are currently being analyzed for mutations in the Merlin gene. Preliminary data has indicated that the Merlin gene may not be rearranged in all sporadic acoustic neuromas (R.K. Wolff, personal communication), suggesting that other chromosome 22 genes may be involved in the development of these tumors.

As part of an ongoing effort to identify genes involved in the development of acoustic neuromas, we have previously described the analysis of a sporadic acoustic neuroma containing a chromosome 22 translocation approximately 2 Mb distal to the Merlin gene, between D22S347 and D22S349 (Frazer et al. 1993). Other workers have also reported chromosomal rearrangements in acoustic neuromas and in a meningioma in approximately the same region of

chromosome 22 containing the translocation. As we immortalized the translocated chromosome 22 in a hamster-tumor somatic cell hybrid, we were able to sequence the Merlin gene that was present in the tumor. This sequence analysis has indicated that the primary structure of the Merlin gene remaining in the sporadic acoustic neuroma was not mutated (R.K. Wolff, unpublished data). These data combined with the observation that other sporadic tumors also appear to contain rearrangements in the same region of chromosome 22, suggest that the translocation alters the expression or function of a second chromosome 22 locus involved in the development of acoustic neuromas.

The identification of several disease genes by positional cloning has been greatly aided by either a germline or somatic cell translocation(s) involving the gene (Viskochil et al., 1990, Davies K, 1993). A useful approach in isolating a gene defined by a translocation breakpoint is to segregate the derivative chromosome homolog away from the structurally normal chromosome homolog in a somatic hybrid cell line. A map of ordered DNA markers can then be used to determine the closest flanking loci of the translocation breakpoint by simply scoring for their presence or absence in the hybrid cell line carrying the derivative chromosome. This approach then involves isolating the genomic region between the flanking DNA markers to generate new markers, which can then be used to further narrow the region containing the translocation breakpoint. In practice, new DNA markers are generated until a probe is obtained that identifies a restriction fragment altered by the translocation, using Southern blot analysis. The detection of altered restriction fragments with a variety of different enzymes provides strong evidence that the probe maps close to the translocation breakpoint. To find transcribed sequences altered by the translocation, this probe is then either used to screen cDNA libraries directly

(Volpe et al., 1993), or as a reagent to isolate cloned "trapped exons" by exon amplification (Buckler et al., 1991, Trofatter et al., 1993) or by exon trapping (Duyk et al., 1990).

One of the difficult aspects of this positional cloning strategy is the isolation of the genomic region between the flanking DNA markers. Currently, most workers use yeast artificial chromosome (YAC) libraries to isolate large cloned fragments (200 kb - 1 Mb) of DNA from the genomic region of interest, by hybridization or PCR screening. A contiguous set of overlapping YAC clones (i.e. a contig) is constructed by analyzing the DNA content, size and ends of the YACs. Recently, as a method of characterizing the YACs and converting them into cosmids, YAC clones have been used as probes to screen chromosome specific cosmid libraries. Comparison of the cosmids hybridization patterns with a number of overlapping YACs allows one to group the cosmids into defined regions (referred to as a bin). The cosmids within a bin are not ordered relative to each other and if the YACs contain deletions or if there are genomic regions not represented in the cosmid library, the cosmids within the same bin may not be overlapping. A contig of the cosmids within each bin and between adjacent bins can be constructed by comparing the Eco R1 restriction patterns of the cosmids and by using the cosmid clones as probes to screen the chromosome specific cosmid library.

In this chapter, I describe my efforts to isolate the chromosome 22 gene, distal to Merlin, involved in the development of acoustic neuromas. The closest flanking DNA markers, D22S347 and D22S349, of the translocation that interrupts this gene are separated by approximately 250 kb (Frazer et al., 1993). To develop new markers closer to the translocation breakpoint, I screened YAC libraries with STSs at the D22S347 and D22S349 loci. I isolated six YAC

clones which I used as probes to screen a sub-chromosome 22 specific cosmid library. The cosmids isolated with the YACs at the D22S347 locus were placed into 6 separate bins, spanning a distance of approximately 350 kb. Screening the cosmid library with the YACs at the D22S349 locus combined with YAC end and cosmid hybridization experiments, resulted in an ordered array of cosmids consisting of 8 bins that also span a distance of approximately 350 kb. These two sets of binned cosmids at the D22S347 and D22S349 loci did not overlap with each other, however my data indicates that the breakpoint is most likely located within 50 kb of the cosmids in the left end bin at the D22S349 locus.

Materials and Methods:

PCR Oligonucleotides

The PCR conditions and primers for the D22S347 (RW3-8) and the D22S349 (RW3-20) chromosome 22 loci have been previously described. (Frazer et al., 1993).

YAC libraries and Screening

The YAC libraries used in this study were constructed at the Washington University Medical School, St. Louis (Imai and Olson, 1990) and at CEPH, Paris (Albertson et al., 1990). The Washington University library was screened using a combination of PCR and hybridization. The positive YAC clones were localized to a single batch of DNA pooled from a set of 384 YAC clones (four 96 well microtiter plates of the gridded YAC library), by analyzing pools of YAC DNA with PCR. The individual positive YAC colony was then identified by hybridization of the DNA probe to membranes containing DNA isolated from the 384 YAC colonies in the positive pool (Green and Olson, 1990). The CEPH library was screened entirely by PCR. A positive YAC clone was localized to a single pool of 96 YAC colonies by PCR analysis, in the same manner described above for the Washington University library. DNA pools of the rows and columns from the positive microtiter plate were then screened by PCR to identify the individual positive clone.

YAC Characterization

After identification, the individual positive clones were maintained in selective media as described (Burke et al., 1987). Each positive clone was

streaked and at least six subclones were analyzed by PCR to determine if they contained the YAC. The PCR analysis was performed as follows: a small amount of each subclone was scraped off the media plate with a toothpick and mixed with 1.6 μmoles of each deoxyribonucleoside triphosphate, 10 ρmoles of each oligonucleotide primer, 0.25 units of *Thermus aquaticus* DNA polymerase, in 10 μl PCR buffer (2.5 mM $MgCl_2$, 50 mM KCl, 20 mM Tris-Cl, pH 8.3). The samples were overlaid with mineral oil and incubated at 94°C, 62°C, and 72°C for 1 minute at each temperature in an automated Cetus-Perkin Elmer Thermal Cycler for a total of 35 cycles. Yeast chromosomes were prepared in agarose blocks according to standard procedures and fractionated by pulse field gel electrophoresis (PFGE) analysis on a Bio-Rad CHEF Mapper™, using conditions recommended by the vendor to separate DNA in the 90 kb to 1 Mb range. Yeast chromosomes from the YP148 strain were used as size standards on all gels. The fractionated yeast chromosomes were transferred to nylon membranes (Hybond N+; Amersham), hybridized with radioactive probes, washed, exposed to Kodak XAR film, and stripped of probe prior to rehybridization, as previously described (Wolff et al. 1992).

YAC End Isolation

The terminal sequences of the YAC clones were isolated by Alu-Vector PCR using combinations of the two Alu primers, ALE3 (5'-CCA(C/T)TGCACTCCAGC CTGGG-3') and PDJ34RP (5'-CCCAGGCTGGACA(G/A)TGG(T/C)(A/G)(T/C) (A/G)ATC(A/T)(T/C)(A/G)GCTCA-3'), with the two vector primers, ODC 333 for the left arm, and ODC 334 for the right arm (Zuo et al., 1992). Alu-Vector PCR products were compared with the PCR products of the Alu primers used alone to distinguish the terminal YAC sequences from the internal Alu-Alu bands.

Reactions were performed as follows: agarose blocks of the yeast strains containing the YACs were melted at 50°C, a 5 μl aliquot was mixed with 20 μmoles of each deoxyribonucleoside triphosphate, 50 pmoles of each oligonucleotide primer, 2.5 units of *Thermus aquaticus* DNA polymerase, in 100 μl PCR buffer (1.5 mM $MgCl_2$, 50 mM KCl, 20 mg/ml gelatin, 10 mM Tris-HCl, pH 8.4). The samples were overlaid with mineral oil and incubated at 94°C for 1 minute, 55°C for 1 minute and 72°C for 2 minutes in an automated Cetus-Perkin Elmer Thermal Cycler for a total of 30 cycles. The reaction products were fractionated on a 1.5 % LMP agarose (Seaplaque GTG), the specific Alu-vector bands were excised, the gel slice was melted at 50°C, and a 5 μl aliquot was labeled directly with ^{32}P dCTP by random priming at 37°C for 3 hours (Feinberg and Volgelstein, 1984).

Inverse PCR was performed to isolate YAC ends as described (Zuo et al., 1992). The left end of C23-01 H11 YAC was isolated using this approach. The reaction product was cut out of a 1.5% LMP agarose (Seaplaque GTG) gel and labeled in the same manner as the Alu-vector PCR bands.

Cosmids corresponding to the ends of several of the YAC clones were identified by screening the sub-chromosome 22 specific cosmid library with overlapping YACs, as described below. The cosmids were grouped into bins, based on their hybridization patterns with the overlapping YACs. The cosmids which hybridized with only one YAC clone were usually located in the left or right end bins. The cosmids in these left or right end bins were assumed to correspond to the terminal sequences of the YAC clone which identified them by hybridization.

Cosmid Library

A cosmid library was constructed from a radiation hybrid, RH130a, which contains a single contiguous fragment of chromosome 22, spanning approximately 9 Mb from D22S1 to PDGF (Frazer et al., 1991). Partial Sau3A digests of RH130a were cloned into the BamH1 site of the pWE 15 vector (Stratagene) and transformed into the *E. coli* strain 490A as described (Wolff et al., 1989), resulting in approximately $1x10^5$ primary colonies. To determine which of these cosmids contained human chromosome 22 DNA, the entire library was screened with ^{32}P dCTP-labeled total human DNA and then with ^{32}P dCTP-labeled total hamster DNA as described (Wolff et al., 1992). Based on specific hybridization with the total human DNA probe, a total of 957 independent cosmids were transferred into 11 microtiter plates. These cosmids were replicated onto nylon filters, each of which contained 384 colonies from 4 microtiter plates.

Screening with YAC DNA

YAC DNA was excised from a 1.3 % LMP agarose (Seaplaque GTG) after being fractionated by PFGE, as described above. The gel slices containing the YAC DNA were treated with β-agarase (NEB), precipitated with isopropanol, extracted 3 times with phenol/chloroform, precipitated with ethanol, and then resuspended in 50 µl of TE pH 8.0. Approximately 500 ng of YAC DNA was labeled with ^{32}P dCTP by random priming to a specific activity of 5×10^8 cpm/µg. The labeled YAC DNA was mixed with 60 µg pYAC4 vector DNA, and 400 µg human Cot1 DNA in 700 µl of TE pH 8.0. The probe mixture was boiled for 5 minutes, transferred to 65°C, immediately thereafter 100 µl 1M $NaPO_4$ pH 7.4 was added, and the incubation continued at 65°C for 2 hours. The cosmid

filters were prehybridized for at least 2 hours at 65°C in 7 % SDS, 0.25 M $NaPO_4$ pH 7.4, 1 mM EDTA, and 250 μg/ml sheared salmon sperm DNA. The probe mixture was added to the buffer used for prehybridization and the filters were hybridized overnight. Filters were washed three times, 25 minutes each, at 65°C with 0.3X SSC, and 0.1 % SDS, and exposed to Kodak XAR film at -70°C for 5-12 hours.

Cosmid Preparation

Cosmid DNA was isolated by alkaline lysis using standard procedures (Sambrook et al., 1989). To isolate the insert as a single large fragment, the cosmid DNA was digested with Not I, electrophoresed on a 0.5 % LMP agarose gel (Seaplaque GTG) for 15 hours at 40 volts, ethidium stained, and the insert fragment excised out of the gel. The gel slice containing the insert was melted at 50°C and a 5 μl aliquot was labeled directly with ^{32}P dCTP by random priming at 37°C for 3 hours.

DNA Extraction Southern Blotting and Hybridization

High-molecular-weight DNA was isolated from tumor tissue, lymphoblastoid cell lines, and hamster-tumor hybrids, digested to completion with restrictions enzymes, fractionated by electrophoresis, transferred to nylon membranes (Hybond N+; Amersham), hybridized with ^{32}P dCTP-labeled probes, washed, exposed to Kodak XAR film, and stripped of probe prior to rehybridization, as previously described (Wolff et al. 1992).

Results

YAC isolation and characterization

To isolate the chromosome 22 locus distal to Merlin that is involved in the development of sporadic acoustic neuromas, I attempted to clone the estimated 250 kb genomic region between the DNA markers, D22S347 and D22S349, which flank a translocation breakpoint that affects this gene (Frazer et al., 1993). Since the yeast artificial chromosome (YAC) cloning system allows the cloning of large DNA inserts, I used STSs from the D22S347 and D22S349 loci to screen two different YAC libraries,Washington University and CEPH, as described in Materials and Methods. The mean YAC size is 380 kb in the Washington University library (Imai et al., 1990) and 430 kb in the CEPH library (Albertson et al., 1990). Therefore, the 57,000 individual YAC clones screened comprise approximately seven-to eight-fold coverage of the human genome. In total, I isolated four YACs with the D22S347 STS and two YACs with the D22S349 STS. Single colonies of each of these YAC strains were prepared in agarose blocks and fractionated by PFGE. After blotting the gels, we determined the size of the YAC clones by hybridization with YAC vector sequences (Figure 1). The insert sizes of the YACs ranged from 350 kb to 500 kb, with an average size of 380 kb.

Screening the Cosmid Library Directly with YACs

To characterize the six YACs for their content of chromosome 22 material and to determine their extent of overlap with each other, I screened a sub-chromosome 22 specific cosmid library by using the YAC clones as hybridization probes. The cosmid library was constructed from radiation hybrid RH130a, as described in Materials and Methods. On the basis of probe content

mapping and in situ hybridization analysis, the only human material present in hybrid RH130a is a contiguous 9 Mb fragment of chromosome 22, which includes the region between the D22S347 and D22S349 loci. The average size insert of the cosmids in this library is approximately 38 kb. Therefore, we estimate that the 957 independent colonies represent a three-fold coverage of the 9 Mb fragment of chromosome 22 present in hybrid RH130a. The DNA sequences for the D22S347 and D22S349 STSs were obtained from cosmids (P310C and P43C) isolated from this library. When the cosmids at the D22S347 and D22S349 loci were used as probes to screen the sub-chromosome 22 specific library, they hybridized with a total of 3 and 4 cosmids, respectively (Tables 1 and 2c). These data supports our estimate of the cosmid library representing a three-fold coverage of the 9 Mb region of chromosome 22. A total of 56 different cosmids were isolated by screening this library with the 6 YACs. For each YAC probe, two types of positive signals were observed. Some of the cosmids had strong positive signals while other cosmids had weak positive signals (Figure 2). Cosmids hybridizing with more than one YAC clone in general consistently had either strong or a weak positive signals with each of the YACs.

Localization of the cosmids by binning

The cosmids were localized into bins, by comparing their hybridization patterns with the overlapping YAC clones (Figure 3, Tables 1 and 2a). The four YAC clones isolated with the D22S347 STS hybridized with a total of 29 different cosmids, which were divided into six separate bins (Table 1). Based on an average cosmid insert size of 38 kb and a three-fold coverage library, the 29 cosmids ordered within bins at the D22S347 locus probably span a distance

of 350 kb. This approach of organizing the cosmids into bins enabled us to determine which of the YACs have overlapping inserts (Figure 3, Tables 1 and 2a). Since the D22S347 and D22S349 loci are separated by approximately 250 kb and the average size of the YACs isolated was 380 kb, I had expected that the YAC clones isolated with the D22S347 and D22S349 STSs would overlap with each other. However, the two YACs isolated with the D22S349 STS hybridized with 27 cosmids, none of which had hybridized with the YACs isolated with the D22S347 STS. These 27 cosmids were originally binned into three groups based on their hybridization patterns with the D22S349 YACs (Table 2a).

Isolation and Characterization of YAC Ends.

To refine the location of the cosmids within the end bins and to further characterize the YACs, I isolated the ends of the YAC clones by Alu-vector PCR and inverse PCR, to use as probes to screen the sub-chromosome 22 specific cosmid library. Using the Alu-vector PCR approach I successfully isolated 4 ends from 6 different YAC clones. I used the inverse PCR approach on 2 different YAC clones and isolated 1 end. The results of the isolation and characterization of these YAC ends are summarized in Table 3.

The left and right ends isolated from the D22S349 YAC, A21-06 G6, hybridized with cosmids in the sub-chromosome 22 specific library, indicating that the entire YAC insert is derived from this region on chromosome 22 (Tables 2b and 3). The right end of YAC A21-06 G6 hybridized with a cosmid (P69E) that I had originally placed within the middle bin at the D22S349 locus (Tables 2a and 2b). This cosmid was originally localized in the middle bin because it hybridized with both D22S349 YACs, A21-06 G6 and 233B10. Because of the

fact that many YACs are known to contain internal rearrangements, I believe that this cosmid is most likely located at the right end of YAC A21-06 G6 and that YAC 233B10 has an internal deletion (Table 2b). This demonstrates that the approach of binning the cosmids based on their hybridization patterns with overlapping YACs can be misleading. In this case, a YAC containing an internal deletion apparently introduced errors in the cosmid order, by placing cosmids within a middle bin that should have been placed within an end bin.

The Alu-vector PCR product for the left end of YAC A21-06 G6 was relatively small (230 bp) but hybridized with five cosmids, three of which had not been detected screening with the whole YAC A21-06 G6 (Tables 2a and 2b). This result may be due to the fact that I pre-annealed the labeled YAC probes with an excess of unlabeled YAC vector to reduce the background signal caused by vector-vector hybridization. The hybridization signals of the sequences at the very end of the human DNA insert may also have been reduced by this procedure. Two of the cosmids (P11 6H, P10 2F) which hybridized with the left end of YAC A21-06 G6 were located in the middle bin, two of the cosmids (P9 11H, P9 11G) were located in the left end bin, and one cosmid (P11 7E) had not previously been detected screening with either of the YACs at the D22S349 locus (Tables 2a and 2b). These data confirmed the placement of the P9 11H and P9 11G cosmids in the end bin and sub-localized the positions of the P11 6H and P10 2F cosmids in the middle bin. As shown in Tables 2b and 2c, the fact that YAC 233B10 hybridized with cosmid P49G, but did not hybridize with cosmid P117E, suggest that it may also contain a small internal deletion at the left end.

Two of the YAC ends amplified by Alu-vector PCR and the one YAC end isolated by inverse PCR did not hybridize with cosmids in the sub-chromosome

22 specific library (Table 3). These results suggest that the D22S347 YACs from which they were derived, C32-10 H11 and 498H2, are chimeric. However, I have not ruled out the possibility that the isolated YAC ends are from this region on chromosome 22, but were not represented in the sub-chromosome 22 specific cosmid library.

This approach of isolating YAC ends to confirm and further refine the location of the cosmids in the end bins worked well at the D22S349 locus; however, it was unsuccessful at the D22S347 locus. I was not able to isolate any YAC ends to confirm the location of the cosmids in the left and right end bins at the D22S347 locus. Therefore, I assumed that the cosmids were correctly placed in these end bins based on their hybridization patterns with the overlapping D22S347 YACs (Table 1). Although rearranged YACs can incorrectly localize cosmids within bins, I screened the chromosome 22 specific cosmid library with four overlapping YACs at the D22S347 locus, and therefore believe that the probability of errors in the cosmid order due to internally deleted YACs is minimal.

Refinement of cosmid orders by restriction digests and hybridization analysis.

To further establish the extent of overlap between cosmids located within the end bins, I determined their Eco R1 restriction patterns. The cosmids were digested with Eco R1, fractionated in an 0.8% agarose gel, and the ethidium-stained banding patterns between the cosmids in each end bin were compared. The five cosmids placed in the left end bin at the D22S347 loci were divided into two groups based on their Eco R1 restriction fragments; cosmids P11A, P104H and P104G had at least 80 percent overlap, and the cosmids P111D, and P111E had approximately 90 percent overlap with each other (Table 1).

However, these two groups of cosmids located within the same bin, did not have any Eco R1 bands in common. The two cosmids located in the right end bin of the D22S347 contig, P113G and P27B, shared approximately 50 percent of their restriction fragments in common with each other (Table 1).

The Eco R1 restriction fragments of the five cosmids that had hybridized with the left end of YAC A21-06 G6 were also analyzed to determine their amount of overlap with each other. Based on the comparison of their Eco R1 banding patterns two of the cosmids, P911G and P911H, are identical, the cosmid order, P102F-P911G-P117E, was confirmed and one cosmid, P116H, did not overlap with the other cosmids (Table 2b).

To further refine the positions of the cosmids at the D22S349 locus, I used cosmids located within the end bins as probes to screen the sub-chromosome 22 specific cosmid library. The two cosmids, P102F and P911H, located within the left end bin hybridized with the same six cosmid clones, one of which (cosmid P63G) had not been previously detected (Table 2c). These data established a new left end bin at the D22S349 locus, containing a single cosmid (P63G) (Table 2c). The cosmid within the right end bin (P69E) hybridized with itself and with one other cosmid (P11D). This result defined a new bin, containing cosmid P11D, to the right of the large internal deletion in YAC 233B10 (Table 2c).

Localization of the YAC contigs in relationship to the chromosome 22 translocation breakpoint.

My initial objective was to clone the genomic region between the D22S347 and D22S349 loci, to obtain a probe that detected restriction fragments altered by the translocation. Although the YAC clones at the D22S347 and D22S349

loci did not overlap with each other, it was possible that one of the sets of YACs crossed the translocation breakpoint. If either of the YAC contigs at the D22S347 or the D22S349 loci spanned the translocation, it would provide the necessary cloned material to detect and analyze the breakpoint.

To determine if the D22S347 YAC contig crossed the translocation breakpoint, I hybridized two cosmids from the left end bin P11A and P111D, and one cosmid located within the right end bin, P113G, to Southern blots containing genomic DNA isolated from the hamster-tumor hybrid, A6-1, that captured the translocated chromosome, as well as from hamster-tumor hybrids which contained a normal copy of chromosome 22. All three of these cosmids displayed normal hybridization patterns in the hybrid A6-1, indicating that the entire D22S347 YAC contig is proximal to the translocation (Figure 4).

I next established whether the D22S349 YAC contig crossed the translocation breakpoint. I hybridized the Southern blot containing the translocated chromosome 22 with two cosmids from the left end, P102F and P911H, and the one cosmid, P69E, within the right end bin. None of these cosmids identified any restriction fragments in the hybrid, A6-1, containing the translocated chromosome, indicating that the entire D22S349 YAC contig is located distal to the breakpoint.

Discussion

I am interested in isolating and characterizing genes involved in the development of nervous system tumors. In this chapter I describe my efforts to clone a chromosome 22 translocation breakpoint that interupts the expression of gene most likely involved in the development of sporadic acoustic neuromas.

Strategies for isolating disease genes based on their chromosomal position generally rely on cloning large regions of genomic DNA between two flanking loci. In this study, the closest flanking DNA markers of the translocation breakpoint, D22S347 and D22S349, are separated by approximately 250 kb. The ability to clone segments of genomic DNA of this size has been greatly facilitated by the development of human YAC libraries, which contain clones with large DNA inserts. A YAC contig spanning the region between the flanking loci, D22S347 and D22S349, would provide the necessary cloned materials for the identification of the breakpoint. However, YAC clones are often difficult to analyze and manipulate. A major problem in using YACs is that approximately fifty percent of the clones in most libraries are chimeric, such that a considerable amount of the DNA in a set of overlapping YAC clones is not from the genomic region under study. In addition, isolating DNA directly from YACs is time-consuming and usually only small quantities of DNA are obtained. To solve these problems, I converted the YAC clones isolated with STSs at the loci D22S347 and D22S349 into cosmids, which are more easily analyzed and manipulated. Since the YACs were used as probes to directly screen a sub-chromosome 22 specific cosmid library, I required only small quantities of YAC DNA and was quickly able to access the chromosome 22 material present in the chimeric YAC clones.

In agreement with other studies my results indicate that this procedure of using labeled YAC DNA to directly screen a chromosome specific cosmid library is an

efficient method of converting the YAC clones into cosmids. When cosmids located within the middle bins were used as probes to screen the library, all the positive cosmid clones had previously been identifed by screening with the YACs. These data suggest that this approach most likely identifies the majority of the cosmids corresponding to the YAC clones.

Each YAC probe was observed to have two types of positive cosmid signals, strong and weak. The fact that cosmids hybridizing with more than one YAC clone in general consistently had either weak or strong signals, indicates that differences in the signal intensities are due to the genomic sequences of the human DNA inserts in the cosmids. One possible explanation of these results is that the genomic DNA complementary to the weak positive cosmids is not easily labled in YACs by the random priming method. Other workers have reported that weak positive signals observed with their primary YAC screens on cosmid libraries were not true positives (Zuo et al., 1993). The differences between their results and mine may possibly be attributed to the fact that I eliminated background signals caused by vector-vector hybridization by prehybridizing the labeled YAC probe with an excess amount of unlabeled YAC vector.

The STSs at the D22S347 and D22S349 loci were used to screen two YAC libraries consisting of seven to eight equivalents of the human haploid genome. In total, I isolated four D22S347 and two D22S349 YAC clones suggesting that this region of chromosome 22 may be underrepresented in these libraries. Based on the average insert size of the YAC clones (380 kb) and the number of YACs obtained, I had expected to observe overlap between the YACs at the D22S347 and D22S349 loci. The fact that I did not observe any overlap suggests that the region of chromosome 22 between these YAC contigs may be prone to deletions in yeast, and is therefore difficult or impossible to clone in YAC vectors. Similiar

observations of other regions of the genome being difficult to clone in YACs have been previously reported (Zuo et al., 1992).

At the D22S347 locus, the cosmids span approximately 175 kb in both directions from the STS used to isolate the YACs (Figure 3). In contrast, at the D22S349 locus, the cosmids span approximately 300 kb in one direction and 50 kb in the other direction from the D22S349 STS. Since the D22S347 and D22S349 STSs are approximately 250 kb apart from each other (Frazer et al., 1993), the cosmids at the D22S349 locus are most likely oriented such that the bins comprising the 300 kb section are distal, and the bins comprising the 50 kb section are proximal to the D22S349 STS. These data indicate the translocation breakpoint that lies between the D22S347 and D22S349 loci, is most likely located within a maximum distance of 50 kb from the cosmids in the left end bin at the D22S349 locus (Figure 3).

The YAC contigs and cosmid bins at the D22S347 and D22S349 loci provide valuable reagents for the isolation of the chromosome 22 gene interrupted by the translocation breakpoint, and the eventual characterization of its role in the development nervous system tumors. The next step in cloning the gene at the breakpoint involves using the cosmids in the end bins as probes to screen the sub-chromosome 22 specific library, in order to obtain a set of overlapping cosmids connecting the YAC contigs at the D22S347 and D22S349 loci. The orientation of the cosmids at the D22S347 locus is unknown. However, the cosmids at the D22S349 locus are oriented such that the left bin is most likely proximal and the right bin distal. Therefore the most efficient method of constructing a contig of the region, would be to initiate the screening of the sub-chromosome 22 specific library using the cosmid located in the left end bin of the D22S349 locus. After a cosmid contig of the region is established, the overlapping cosmids can then be used as

probes on Southern blots containing genomic DNA of the deriviative chromosome 22 to obtain a clone that detects restriction fragments altered by the translocation.

References

Ahmed FB, Maher ER, Affara NA, Bentley E, Xuereb JH, Rouleau GA, Hardy D, David M, Ferguson-Smith MA (1991) Deletion mapping in acoustic neuroma. Cytogenet Cell Genet HGM11:203

Albertson HM, Abderrahim H, Cann HM, Dausset J, Le Paslier D, Cohen D (1990) Construction and characterization of a yeast artificial chromosome library containing seven haploid human genome equivalents. Proc. Natl. Acad. Sci. USA 87:4256-4260.

Buckler AJ, Chang DD, Graw SL, Brook JD, Haber DA, Sharp PA, Housman DE (1991) Exon amplification : a strategy to isolate mammalian genes based on RNA splicing. Proc Natl Acad Sci USA 88:4005-4009.

Burke DT, Carle GF, Olson MV (1987) Cloning of large segments of exogenous DNA into yeast by means of artificial chromosome vectors. Science 236:806-812.

Davies K (1993) Cloning the Menkes disease gene. Nature 361:98.

Duyk GM, Kim s, Myers RM, Cox DR (1990) Exon trapping: A genetic screen to identify candidate transcribed sequences in clones mamalian genomic DNA. Proc Natl Acad Sci USA 87:8995-8999.

Feinberg AP, Volgelstein B (1984) A technique for labeling restriction endonuclease fragments to high specific activity. Anal Biochem 137:266-267

Frazer KA, Boehnke M, Budarf ML, Wolff RK, Emanuel BS, Myers RM, Cox DR (1992) A radiation hybrid map of the region on human chromosome 22 containing the neurofibromatosis type 2 locus. Genomics 14: 574-684

Frazer KA, Wolff RK, Myers RM, Cox DR (1993) Characterization of a chromosome 22 translocation in a sporadic acoustic neuroma: Implications for tumorigenesis. Submitted to ASHG, April 1993.

Green ED, Olson MV (1990) Systematic screening of yeast artificial-chromosome libraries by use of the polymerase chain reaction. Proc Natl Acad Scie USA 87:1213-1217.

Imai T, Olson MV (1990) Second-generation approach to the construction of yeast artificial-chromosome libraries. Genomics 8:297-303.

Jackler RK, Pitts LH (1990) Acoustic Neuroma. Neurosurg Clin North Am 1:199-223

NIH/CEPH Collaborative Mapping Group (1992) A comprehensive genetic linkage map of the human genome. Science258:67-86

Sambrook J, Fritsch EF, Maniatis T (1989) In: Molecular Cloning: A Laboratory Manual. Cold Spring Harbor Laboratory Press, pp. 1.25-1.28.

Trofatter JA, MacCollin MM, Rutter JL, Murrell JR, Duyao MP, Parry DM, Eldridge T, Kley N, Menon AG, Pulasid K, Hasse VH, Ambroae DM, Munroe D, Bove C, Haines JL, Martuza RL, MacDonald ME, Seizinger BR, Short MP, Buckler AJ, Gusella JF (1993) A novel moesin-, exrin-, radixim-like gene is a candidate for the neurofibromatosis 2 tumor suppressor. Cell 72: 791-800

Viskochil D, Buchberg AM, Xu G, Cawthon RM, Stevens J, Wolff RK, Culver M, Carey JC, Copeland NG, Jenkins NA, White R, O'Connell P (1990) Deletions and a translocation interrupt a cloned gene at the Neurofibromatosis Type 1 locus. Cell 62:187-192.

Volpe C, Levinson B, Whitney S, Packman S, Gitschier J (1993) Isolation of a candidate gene for Menkes disease and evidence that it encodes a copper-transporting ATPase. Nature Genetics 3:7-13

Wolff RK, Nakamura Y, White R (1988) Molecular characterization of a spontaneously generted new allele at a VNTR locus: No exchange of flanking DNA sequence. Genomics 3: 347-351

Zhang FR, Delattre O, Rouleau G, Couturier J, Lefrancoid D, Thomas G, Aurias A (1990) The neuroepithelioma breakpoint on chromosome 22 is proximal to the meningioma locus. Genomics 6:174-177

Zuo J, Robbins C, Taillon-Miller P, Cox DR, Myers RM (1992) Cloning of the Huntington disease region in yeast artificial chromosomes. Hum Molec Genet 1:149-159.

Zuo J, Robbins D, Baharloo S, Cox DR, Myers RM (1993) Construction of cosmid contigs of the Huntington disease region of chromosome 4: A model for high-resolution restriction mapping of the human genome. Submitted to Hum Molec Genet

Table 1. Sub-Chromosome 22 Cosmid Library Screen with YACs and a cosmid at the D22S347 Locus

YACs and Cosmid	Size (kb)	Cosmids																										
		P1 11D	P1 11E	P1 1A	P10 4H	P10 4G	P5 2F	P3 5A	P3 1F	P1 3H	P3 9D	P1 6G	P1 8A	P1 8F	P3 10C	P6 5C	P6 7G	P8 10G	P11 8D	P1 7H	P4 2D	P6 1G	P8 4D	P9 4D	P10 2C	P11 3B	P11 3G	P2 7B
335A3	500	X	X	X	X	X	X	X	X	X	X	X	X	X	X	X	X	X	X	X	X	X	X	X	X	X		
416E11	380						X	X	X	X	X	X	X	X	X	X	X	X	X	X	X	X	X	X	X	X		
498H2	400										X	X	X	X	X	X	X	X	X									
C32-01 H11	350											X	X	X	X	X	X	X	X	X	X	X	X	X	X	X	X	X
P3 10C	38														X	X	X											

Table 2a. Sub-Chromosome 22 Specific Cosmid Library Screen with YACs at the D22S349 locus

YACs	Size (kb)	Cosmids																										
		P4 9G	P9 11G	P9 11H	P10 2F	P11 6H	P8 3B	P4 3C	P2 9C	P2 1G	P3 2F	P4 1B	P4 5D	P5 5A	P6 6H	P6 9E	P8 2G	P1 1D	P6 9E	P2 1B	P5 3A	P5 7H	P6 4B	P8 2A	P8 2B	P9 8B	P10 5H	P10 12H
233B10	380	X	X	X	X	X	X	X	X	X	X	X	X	X	X	X	X	X	X									
A21-06 G6	350				X	X	X	X	X	X	X	X	X	X	X	X	X	X	X	X	X	X	X	X	X	X	X	X

Table 2b. Sub-Chromosome 22 Specific Cosmid Library Screen with YACs and YAC ends at the D22S349 locus

YACs and YAC ends	Size (kb)	Cosmids																											
		P4 9G	P11 7E	P9 11G	P9 11H	P10 2F	P11 6H	P8 3B	P4 3C	P2 9C	P2 1G	P3 2F	P4 1B	P4 5D	P5 5A	P6 6H	P6 9E	P8 2G	P1 1D	P2 1B	P5 3A	P5 7H	P6 4B	P8 2A	P8 2B	P9 8B	P10 5H	P10 12H	P6 9E
233B10	380	X	*	X	X	X	X	X	X	X	X	X	X	X	X	X	X	X	X	*	*	*	*	*	*	*	*	*	X
A21-06 G6	350					X	X	X	X	X	X	X	X	X	X	X	X	X	X	X	X	X	X	X	X	X	X	X	X
Left end	0.23		X	X	X	X	X																						
Right end	1																												X

Table 2c. Sub-Chromosome 22 Specific Cosmid Library Screen with YACs, YAC ends and cosmids at the D22S349 locus

YACs and Cosmids	Size (kb)	Cosmids																											
		P6	P4	P11	P9	P9	P10	P11	P8	P4	P2	P2	P3	P4	P4	P5	P6	P6	P8	P2	P5	P5	P6	P8	P8	P9	P10	P10	P1	P6
		3G	9G	7E	11G	11H	2F	6H	3B	3C	9C	1G	2F	1B	5D	5A	6H	9E	2G	1B	3A	7H	4B	2A	2B	8B	5H	12H	1D	9E
233B10	380		X	*	X	X	X	X	X	X	X	X	X	X	X	X	X	X	X	*	*	*	*	*	*	*	*	*	X	X
A21-06 G6	350						X	X	X	X	X	X	X	X	X	X	X	X	X	X	X	X	X	X	X	X	X	X	X	X
Left end	0.23			X	X	X	X	X																						
P4 3C	38							X	X	X	X																			
P10 2F	38	X	X	X	X	X	X																							
P9 11H	38	X	X	X	X	X	X																							
Right end	1																													X
P6 9E	38																												X	X

Note: The cosmids and YACs are named based on their position in the library from which they were isolated. The Washington University library YACs have either A21 or C32 in the beginning of their name. All of the other YACs were isolated from the CEPH library. In Table 2b, the Alu-vector PCR amplified left and right ends of YAC (A21-06 G6), are designated as left end and right end, respectively. An X represents positive hybridization, a blank space represents negative hybridization, a * represents negative hybridization likely to be due to a deletion in the YAC.

Table 3. Isolation and Characterization of YAC ends

YAC end	Locus	Method of isolation	Approximate size of PCR product (kb)	Present in sub-chromosome 22 specific library
A21-06 G5 L	D22S347	Alu-vector PCR	0.2	Yes
A21-06 G5 R	D22S347	Alu-vector PCR	1.0	Yes
C32-01 H11 R	D22S349	Alu-vector PCR	0.02	No
498H2 L	D22S349	Alu-vector PCR	0.7	No
C32-01 H11 L	D22S349	Inverse PCR (Nla IV)	0.2	No

Note: In the YAC end column, L stands for the left end and R stands for the right end. For YAC C32-01 H11 the left end was isolated with the Nla IV enzyme digest for inverse PCR.

Figure Legends

Figure 1. A. Ethidium-stained pulse field gel of the six YACs isolated using STSs at the D22S347 and D22S349 loci. The chromosomes of the yeast strain YP148 are used as size standards. B. An autoradiogram showing the hybridization of the cosmid P113G to the YAC clones after transfer of the gel in panel A to a nylon membrane. Since the P113G cosmid clone is only complementary with YAC C32-01 H11, the hybridization signals in all the other lanes are due to cross-hybridization of the cosmid vector sequences with the YAC vector sequences. The multiple bands observed in the lanes containing the YAC clones 498H2, 335A3, and 416E11, are indicative of yeast strains carrying either multiple YACs or YACs that are mitotically unstable. When the cosmid (P310C) corresponding the D22S347 STS was used as a specific hybridization probe, only the largest molecular weight band was observed in each of these yeast strains. Therefore the additional bands are most likely due to the presence of multiple unrelated YACs in the yeast. The band observed in the lane containing yeast strain YP148 is a 1 Mb YAC clone.

Figure 2. An autoradiogram from screening the sub-chromosome 22 specific cosmid library using a YAC (A21-06 G6) at the D22S349 locus as the probe. This filter contains 384 cosmids derived from the four microtiter plates numbered 5-8, in the cosmid library. Notice the two types of positive hybridization signals observed. Cosmids P83B, P55A, and P66H display strong positive signals. In contrast, cosmids P82A,P53A,P82B,P64B, P69E, P82G and P57H display weak positive signals.

Figure 3. A composite map of the region on chromosome 22 between the flanking loci, D22S347 and D22S349, of a translocation breakpoint. The open square and open circle indicate the 22q centromere and telomere, respectively. The YACs used for screening are drawn as lines according to the estimated amount of chromosome 22 material contained within each one, and are named based on the position of the library from which they were isolated (see Table 1 and 2). A cosmid bin is drawn as a series of X's. Cosmids used for characterizing the translocation breakpoint are indicated by name, and their positions within the cosmid bins are indicated.

At the D22S347 locus, I was unable to orient the direction of the YACs and cosmid bins which span approximately 175 kb in both directions from the D22S347 STS. In sections A and B both possible orientations of the YACs and cosmids at the D22S347 locus are shown. At the D22S349 locus, the cosmids span approximately 300 kb in one direction and 50 kb in the other direction from the D22S349 STS. The D22S347 and D22S349 STSs are approximately 250 kb apart from each other (Frazer et al., 1993). Therefore, as shown in section A the cosmids at the D22S349 locus are most likely oriented such that the bins comprising the 300 kb section are distal, and the bins comprising the 50 kb section are proximal to the D22S349 STS.

Figure 4. Southern blot analysis of the hamster-tumor hybrid cell lines containing the translocated and normal chromosome 22. A. An autoradiogram showing the hybridization of a cosmid (P113G) from the right end bin at the D22S347 locus. Lanes 1 contains genomic DNA from hybrid cell line A6-1, which has captured the translocated chromosome 22. Lane 2 contains DNA from hybrid B8-2, which has captured a normal chromosome 22. Cosmid

P113G, as well as, two cosmids from the left end bin P11A and P111D (data not shown), display normal hybridization patterns in hybrid A6-1, indicating that the entire D22S347 YAC contig is proximal to the translocation. B. Autoradiogram of a blot similar to the one shown in panel A, probed with a cosmid (P69E) from the right end bin at the D22S349 locus. Cosmid P69E, as well as, two cosmids from the left end bin P102F and P911H (data not shown) do not identify any restriction fragments in the hybrid A6-1, indicating that the entire D22S349 YAC contig is located distal to the translocation breakpoint.

Figure 1

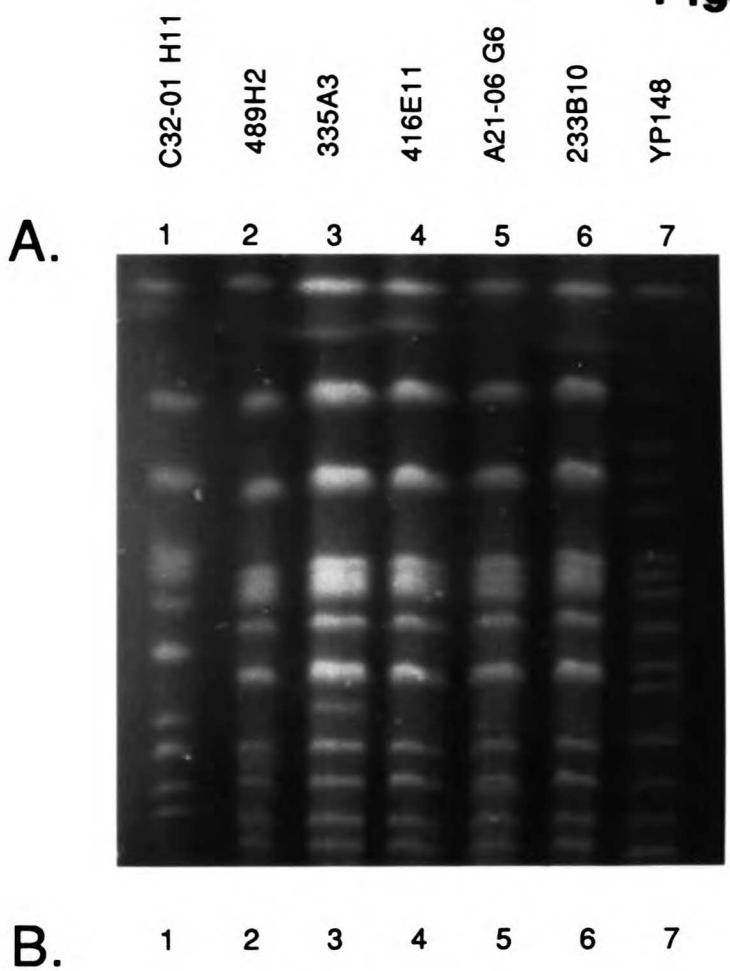
C32-01 H11
489H2
335A3
416E11
A21-06 G6
233B10
YP148
A.
1 2 3 4 5 6 7
B.
1 2 3 4 5 6 7
100

Figure 2

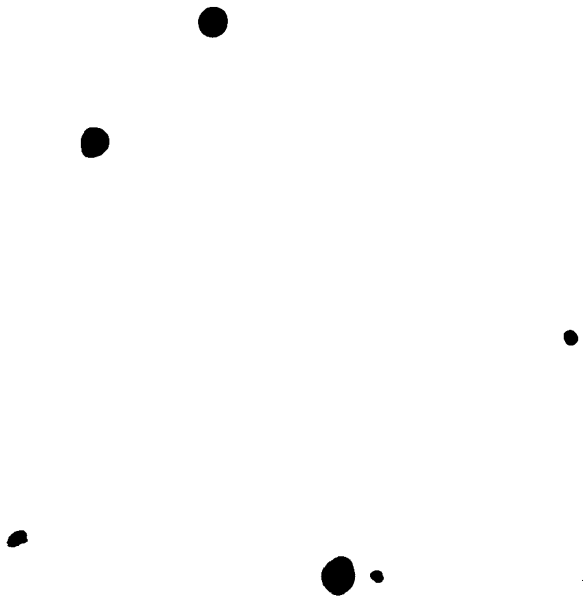

Figure 3

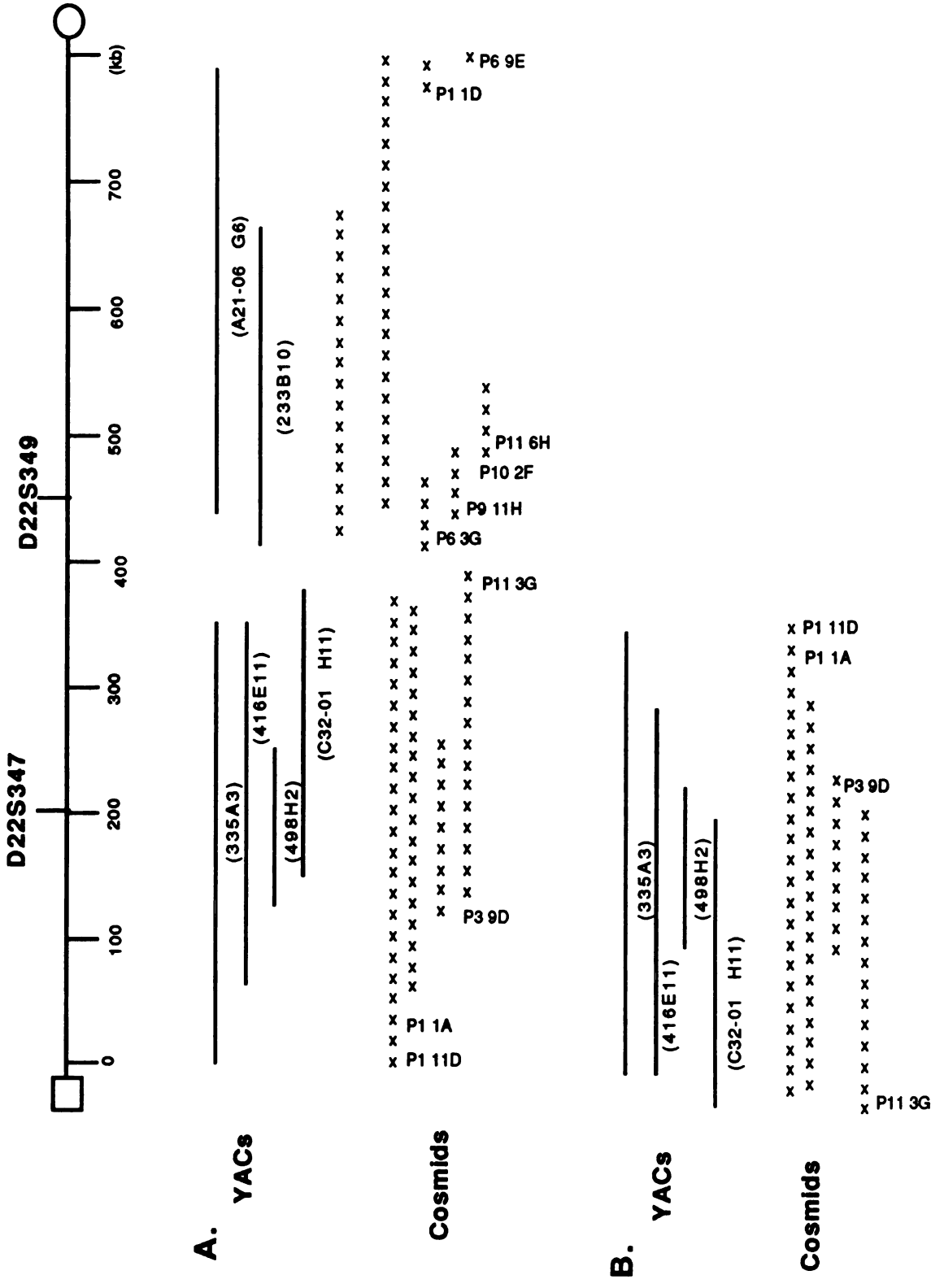
D22S347
D22S349
0
100
200
300
400
500
600
700
(kb)
A.
YACs
(335A3)
(416E11)
(498H2)
(C32-01 H11)
(A21-06 G6)
(233B10)
Cosmids
P1 1A
P1 11D
P3 9D
P11 3G
P6 3G
P9 11H
P10 2F
P11 6H
P1 1D
P6 9E
B.
YACs
(335A3)
(416E11)
(498H2)
(C32-01 H11)
Cosmids
P1 11D
P1 1A
P3 9D
P11 3G

Figure 4

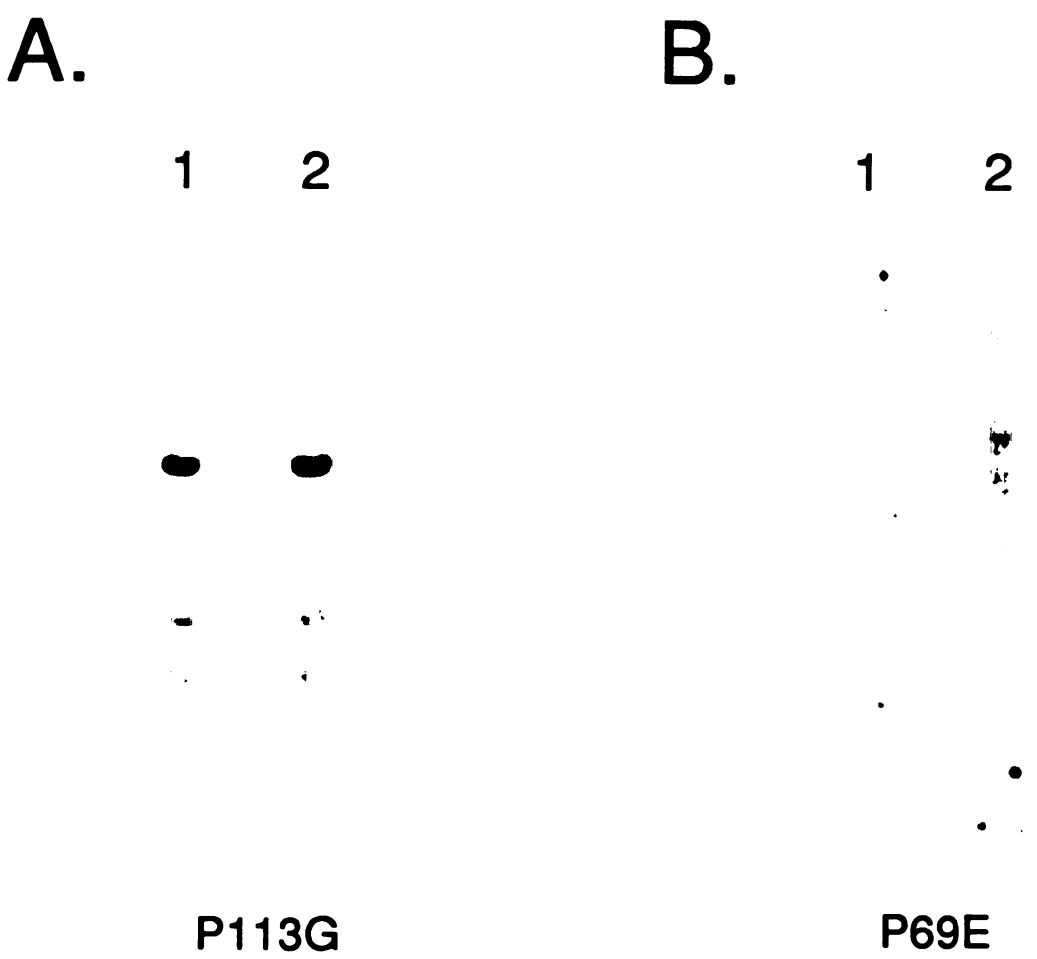

Chapter 5

Summary

At the time I initiated my dissertation research, the NF 2 locus was localized to a 13 cM region on the long arm of chromosome 22, between the DNA markers D22S1 and D22S28. Based on the observation that chromosome 22 DNA was frequently lost in hereditary and sporadic acoustic neuromas, it was assumed that the inactivation of the NF 2 locus was responsible for the development of both classes of acoustic neuromas. However, we realized the possibility that two separate genetic loci, one responsible for the formation of hereditary tumors and the other involved in the development of sporadic tumors, may lie in close proximity to one another on chromosome 22.

The results described in this thesis address the development and application of new techniques used in my effort to isolate the NF 2 gene based on its chromosomal position, and indicate that two genetic loci separated by approximately 2 Mb on chromosome 22 may be involved in the development of acoustic neuromas.

1. A radiation hybrid map of the region on chromosome 22 containing the Neurofibromatosis Type 2 locus.

Chapter one describes a radiation hybrid map at the 500 kb level of resolution of the region on chromosome 22 containing the Neurofibromatosis type 2 (NF 2) gene. A panel of 85 hamster-human somatic cell hybrids containing fragments of human chromosome 22 were generated by x-irradiation and cell fusion. The presence or absence of eighteen human specific chromosome 22 markers was determined in each hybrid by using Southern blot hybridization. We mapped these eighteen chromosome 22 markers by statistically analyzing their cosegregation in these radiation hybrids with two mathematical models; the method of moments and a multipoint maximum

likelihood method. For each model, the framework maps were essentially identical, uniquely ordering eight markers at odds greater than 1000:1. The most likely order of the framework loci is BCR2L - BCR1 - D22S1 - D22S56 - D22S37 - D22S15 - D22S28 - PDGF. The non-framework loci, D22S36, D22S41, D22S33, LIF, D22S44, D22S47, MB and D22S48, were all localized within two adjoining intervals on the framework map at greater than 1000:1 odds. Based on my RH map, the previously defined NF 2 region, D22S1 to D22S28, is estimated to span a physical distance of approximately 6 Mb and is the most likely location for 9 of the 18 markers studied.

2.Characterization of a chromosome 22 translocation in a sporadic acoustic neuroma using a combination of molecular and somatic cell genetic techniques.

Chapter three describes the characterization of chromosome 22 rearrangements in a sporadic acoustic neuroma using a combination of molecular and somatic cell genetic techniques. We analyzed the acoustic neuroma for chromosome 22 deletions or monosomy by comparing the tumor DNA with the patient's blood DNA using 8 polymorphic markers. Three of these markers were heterozygous in the patient's blood DNA and were reduced to hemizygosity in the tumor DNA. Since these 3 markers span approximately one-third the length of the long arm of chromosome 22, these data indicate that the tumor is missing a large part of one chromosome 22 homolog and that it is probably monosomic. To immortalize the chromosome 22 remaining in the tumor, I fused the tumor cells with an established hamster cell line to generate hamster-tumor hybrid cell lines. The resulting hybrid cell line that captured the chromosome 22 derived from the tumor provided an unlimited source for extensive molecular analysis as well as allowed me to karyotype the

chromosome. Analysis of this hybrid cell line by Southern blot hybridization with 17 chromosome 22 loci indicated that the chromosome 22 homolog remaining in the tumor was rearranged in the NF 2 region defined by the flanking markers D22S1 and D22S28. In situ hybridization analysis of the hybrid cell line containing the chromosome 22 derived from the tumor indicated that the chromosomal rearrangement is a reciprocal translocation. I used radiation hybrid mapping to localize the translocation breakpoint to a 250 kb region of chromosome 22, between DNA markers D22S347 and D22S349. Based on my RH map, this region is approximately 2 Mb distal to the recently isolated NF 2 tumor suppressor gene, Merlin. My data, combined with the fact that other workers have also reported chromosome 22 rearrangements 2 Mb distal to the Merlin gene in acoustic neuromas and a meningioma, suggest that the chromosome 22 translocation may alter the expression of a gene involved in the development of these tumors. If this is the case, then at least two different chromosome 22 genetic loci, the Merlin gene and the locus affected by the translocation, are involved in the development of acoustic neuromas.

3. Efforts to isolate the chromosome 22 translocation breakpoint between markers D22S347 and D22S349.

In an attempt to clone the gene affected by the translocation, I isolated DNA from the estimated 250 kb genomic region between the loci that flank the breakpoint, D22S347 and D22S349. Six YAC clones were isolated by screening two YAC libraries with sequence-tagged sites (STSs) generated from the loci D22S247 and D22S249. To establish the order of the YAC clones and to convert them simultaneously into more easily manipulated cosmid clones, I used the YACs as probes to screen a sub-chromosome 22 specific cosmid

library. The isolated cosmids were grouped into defined regions, referred to as bins, based on their hybridization patterns with the overlapping YACs, and were further analyzed by YAC end and cosmid hybridization experiments. The cosmids isolated with the YACs at the D22S347 locus were placed into 6 separate bins, spanning a distance of approximately 350 kb. Screening the cosmid library with the YACs at the D22S349 locus, combined with YAC end and cosmid hybridization experiments, resulted in an ordered array of cosmids consisting of 8 bins that also spans a distance of approximately 350 kb. These two sets of binned cosmids at the D22S347 and D22S349 loci did not overlap with each other. To establish whether either set crossed the translocation breakpoint, I used cosmids located in the left and right end bins at the D22S347 and D22S349 loci as hybridization probes on Southern blots containing the derivative chromosome 22. I determined that neither set of cosmids crossed the chromosome 22 translocation; however, my data indicate that the breakpoint is most likely located within 50 kb of the cosmids in the left end bin at the D22S349 locus. The YAC and cosmid clones at the D22S347 and D22S349 loci provide reagents for isolating the chromosome 22 gene that is affected by the translocation breakpoint and characterizing its role in the development of nervous system tumors.


UC
San Francisco
LIBRARY
UNIVERSITY OF CALIFORNIA · UNIVERSITY OF CALIFORNIA